NAGL-65

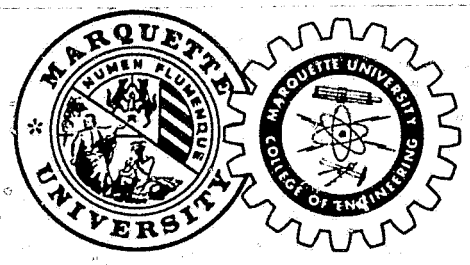

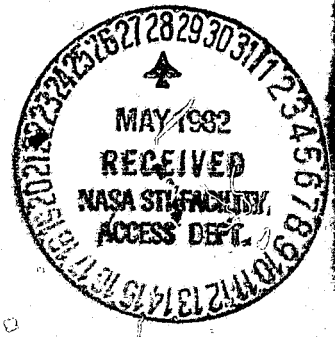

COLLEGE OF ENGINEERING

MARQUETTE UNIVERSITY

MILWAUKEE, WISCONSIN 53233

EFFECT OF WIND GUSTS ON THE MOTION OF A BALLOON BORNE OBSERVATION PLATFORM

NICHOLAS J. NIGRO
ASSOCIATE PROFESSOR

FRANK M. JOHANEK
GRADUATE STUDENT
MECHANICAL ENGINEERING

TABLE OF CONTENTS

CHAPTER I

INTRODUCTION

1.1 Motivation and Relevance of Essay

The balloon system has been employed extensively in the past as a means of conducting research in the earth's atmosphere. The main disadvantage in the use of balloon systems occurs in those experiments where it is necessary to either stabilize the observation platform or use some observer system to perdict its attitude as a function of time. Stabilization or prediction is necessary at times in order to process the experimental data collected by various research instruments which are mounted on the observational platform.

Platform stabilization can be accomplished by means of control systems. However, these systems are usually complex and result in increase cost and additional platform weight which reduces platform payload. Another method is to allow the platform to oscillate freely in space and predict its attitude. Thus, it is important that designers of balloon systems have a understanding of the motion of balloon borne observation platforms in order to determine what kinds of auxilliary systems are necessary for accurate and economical data collection.

The motion of balloon borne observation platforms during ascent and decent have been discussed in several papers (Ref. 1,2). In this essay the effect of wind gusts which result in forces acting externally on the ballooon system will be studied. These forces affect the nature of the motion of

the observation platform while the balloon is at float altitude.

1.2 Objective of Essay

The objective of this essay is to determine the effect of wind gusts on the magnitude of the pendulation angles of a balloon borne observation platform. A system mathematical model will be developed and the solution of this model (in conjuction with data gathered by NASA during a flight mission) will be used to determine the magnitude of the observation platform pendulation angles.

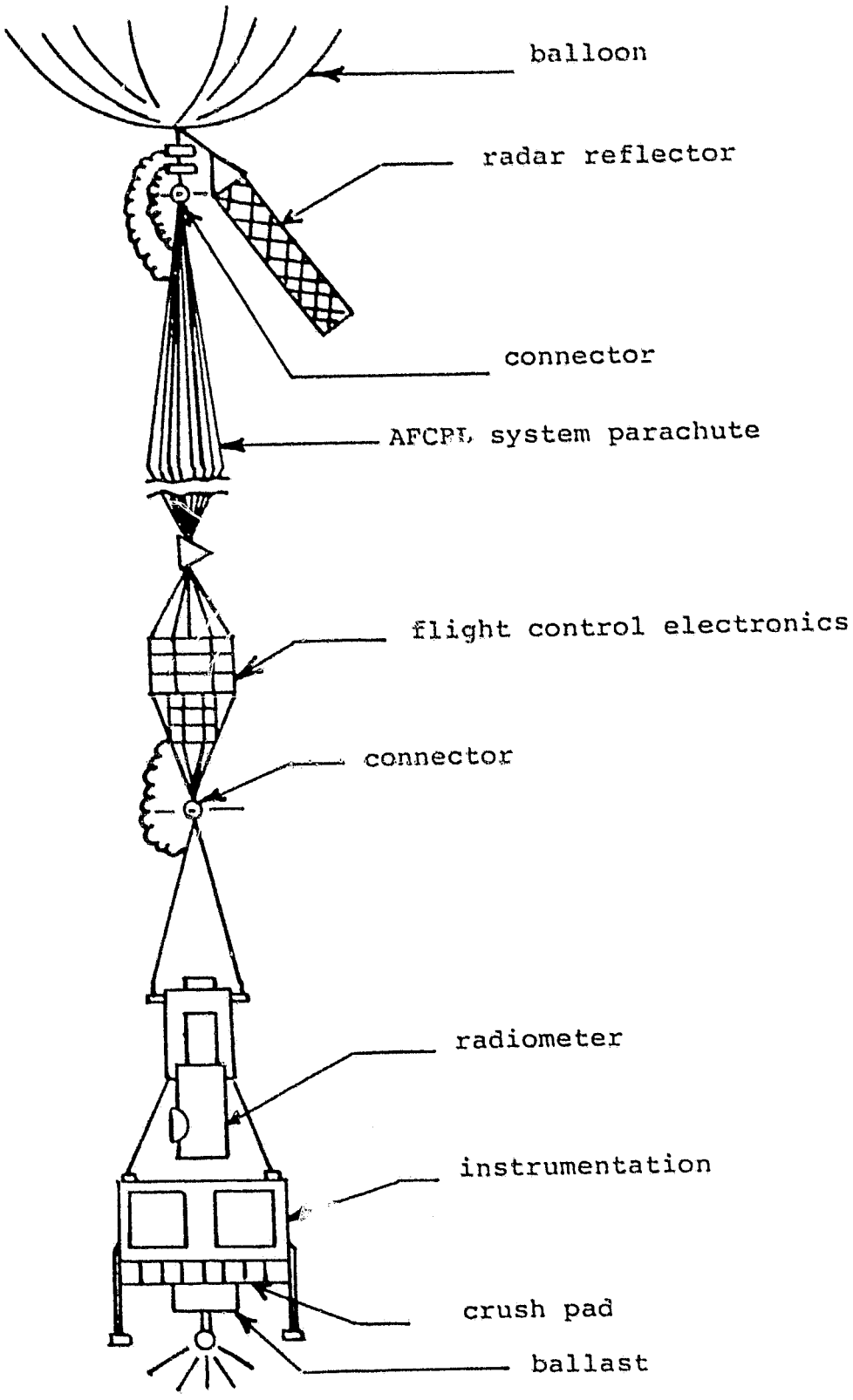

Figure (1) LACATE Balloon System

CHAPTER II

DEVELOPMENT OF MATHEMATICAL MODEL

2.1 LACATE Experiment

The National Aeronautics and Space Administration conducted a high altitude balloon experiment called LACATE (Lower Atmosphere Composition and Temperature Experiment). This experiment employed an infrared radiometer to sense remotely, vertical profiles of concentrations of selected atmospheric trace constituents and temperature.

The balloon system used for the mission is shown in Fig. (1). The system consists of the following:

a. A 39 million cubic feet zero pressure balloon.

b. Radar reflector.

c. Recovery parachute.

d. Flight control electronics.

e. Radiometer.

f. A platform containing the research payload.

When the balloon attained float altitude, data was gathered by the various instruments and telemetered to ground control. The radiometer line of sight was scanned vertically across the horizon at approximately 0.25^{o} per second, requiring 30 seconds to acquire a complete radiance profile. At the end of the mission the platform system was seperated from the balloon and returned to earth by means of the parachute.

2.2 Idealization of Balloon Platform System

The actual motion of the balloon system once it reaches

float altitude is very complex and involves various types of oscillations, including bounce (vertical oscillations), pendulations (in plane motion), spin (rotation), and horizontal translation.

In previous work (Ref. 3) the LACATE system was idealized as shown in Fig. (2). Each balloon subsystem was treated as an equivalent rigid body. The mass of the entire system was lumped at the center of gravity of the balloon and positions 1, 2, and 3 as shown in Fig. (2). Euler angles can be choosen to measure spin and pendulation in two mutually perpendicular planes. It was shown in (Ref. 4) that by choosing the proper set of Euler angles and assuming small displacements the pendulation motion uncouples in two mutually perpendicular planes, thus simplifying the form of the mathematical model. Details of that development can be found in (Ref. 4).

Since the pendulation motion uncouples, the balloon platform system for this study will be further idealized as shown in Fig. (3) in order to develope the form of the system mathematical model. This model in the mutually perpenducular plane (i.e., y-z plane) is the same, with $\theta_1 = \psi_1$ and $\theta_2 = \psi_2$.

For purpose of this study the following assumptions are made:

1. The distributed balloon subsystem will be lumped into two subsystems and treated as equivilant rigid particles.
2. The cables will be treated as inflexible and inextensible.

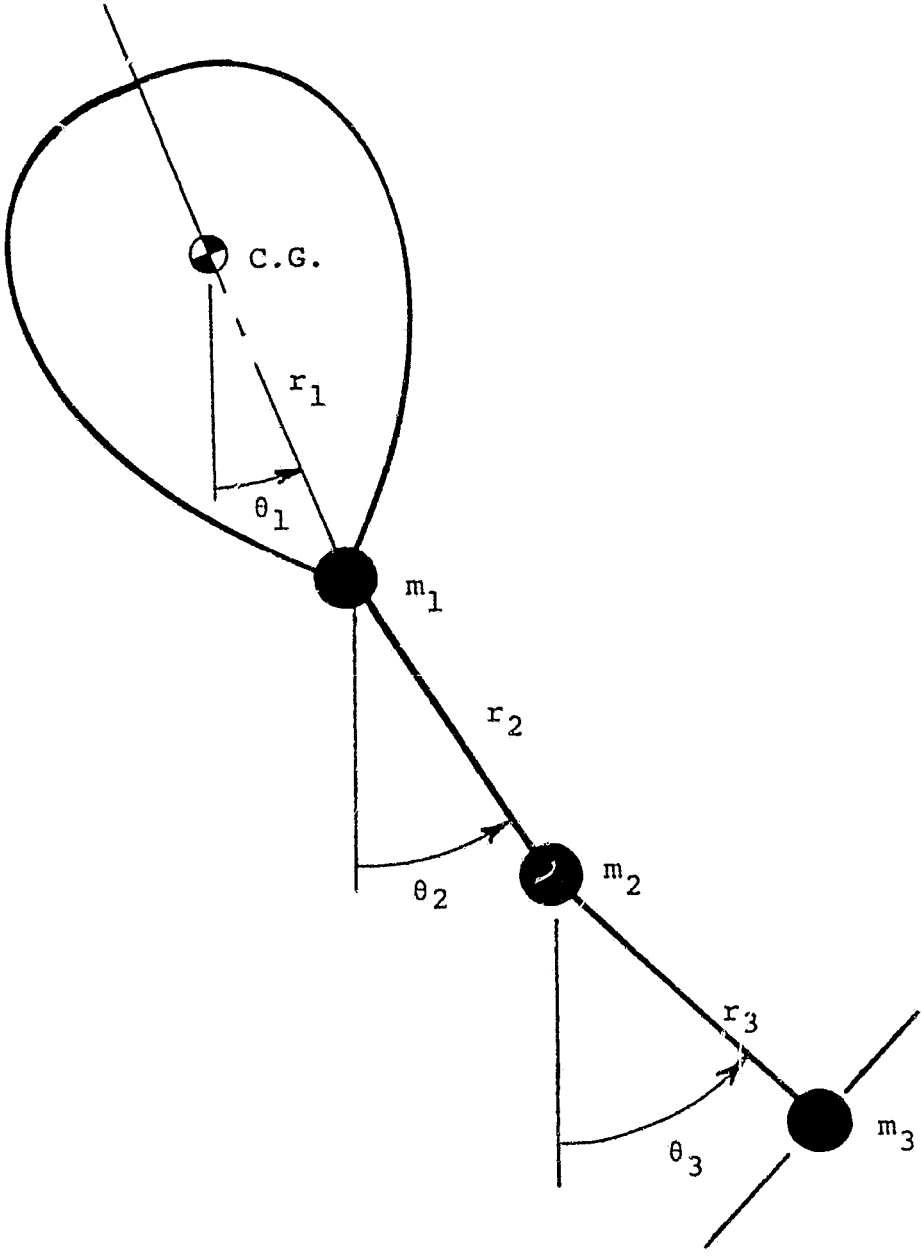

Figure (2) Idealized LACATE System

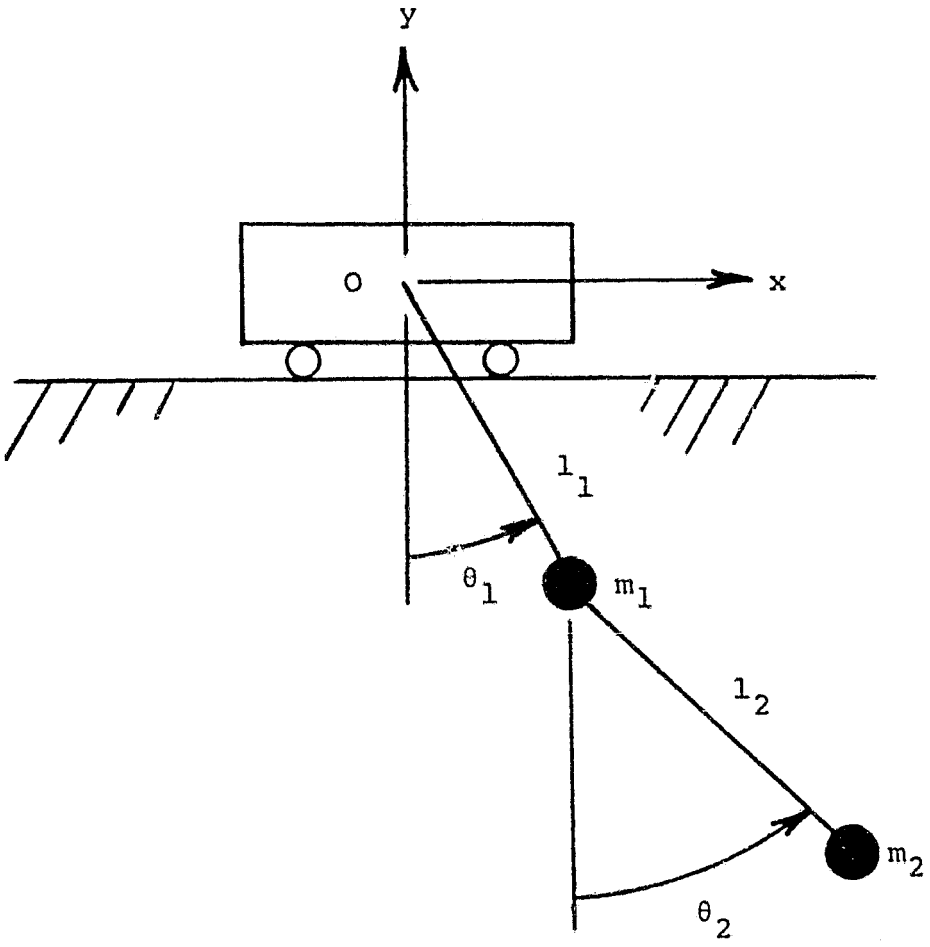

Figure (3) Idealized Balloon Platform System in the x-y Plane

3. The altitude of the support point O will assumed to be constant during the entire period of observation; i.e., $y = 0$.
4. The moments of interia of each subsystem about their center of gravity will be neglected.
5. Viscous drag forces, viscous drag torque and support friction will be neglected.

This idealization enables one to treat the balloon system as a double pendulum with a moving (accelerating) support. The acceleration of the support is due to wind gust forces which act on the balloon. These accelerations cause equivalent excitation forces that affect system response. The main purpose of this work is to study the effect of these forces on the angles θ_1, θ_2, ψ_1, and ψ_2.

2.3 Generalized Coordinates

The generalized coordinates for a given system are those coordinates which are employed to specify the configuration of the system at any instant of time. In any mechanical system the number of degrees of freedom of the system coincides with the minimum number of independent coordinates necessay to describe the system uniquely. In the case of the idealized planar lumped parameter system shown in Fig. (3), two generalized coordinates, angles (θ_1 and θ_2 or ψ_1 and ψ_2) are necessary to specify the configuration. For this study generalized coordinates will be employed in order to facil-

take the use of Lagrange's Equation for developing the mathematical model.

2.4 Lagranges's Equation

The differential equations governing the motion of the system shown in Fig. (3) will be developed by employing Lagrange's equation. The form of the equation used in this study is given as follows; i.e.,

$$\frac{d}{dt}\frac{\partial L}{\partial \dot{q}_k} - \frac{\partial L}{\partial q_k} = Q_k, \qquad k=1,2,\ldots,n \tag{2-1}$$

where

$$\begin{aligned} L &= T - V = \text{Lagrangian}, \\ T &= \text{kinetic energy of the system}, \\ V &= \text{potential energy of the system}, \\ q_k &= \text{generalized coordinate}, \\ \dot{q}_k &= \text{generalized velocity}, \\ n &= \text{number of generalized coordinates, and} \\ Q_k &= \text{the nonconservative generalized forces.} \end{aligned} \tag{2-2}$$

Eq. (2-1) represents a set of n simultaneous differential equations which describe the motion of a holonomic system.

In this study support friction and drag forces are neglected therefore $Q_k = 0$.

The two main advantages for using Lagrange's equation are:

1. The internal reaction forces do no work during the motion and therefore can be neglected.
2. The energy terms can be computed in a straightforward manner.

2.5 System Lagrangian

The kinetic energy of the system shown in Fig. (3) (assuming small angles) is given as follows; i.e.,

$$T = \tfrac{1}{2}m_1(\dot{x} + l_1\dot{\theta}_1)^2 + \tfrac{1}{2}m_2(\dot{x} + l_1\dot{\theta}_1 + l_2\dot{\theta}_2)^2, \quad (2\text{-}3)$$

where

T = kinetic energy of complete system,

m_1 = mass of subsystem 1,

m_2 = mass of subsystem 2,

l_1 = distance from support point O to mass m_1,

l_2 = distance from mass m_1 to mass m_2,

$\dot{x}$ = translation velocity of support point O,

$\dot{\theta}_1$ = angular velocity, and

$\dot{\theta}_2$ = angular velocity.

The potential energy of the system is given as follows:

$$V = m_1 g l_1(1-\cos\theta_1) + m_2 g(l_1(1-\cos\theta_1) + l_2(1-\cos\theta_2)) \quad (2\text{-}4)$$

where

V = potential energy fo the complete system, and

g = acceleration of gravity.

Substitution of Eqs. (2-3) and (2-4) into Eq. (2-2), expanding and simplifing terms yields the system Lagrangian and is given as follows; i.e.,

$$L = \tfrac{1}{2}m_1(\dot{X}^2 + 2L_1\dot{X}\dot{\theta}_1 + L_1^2\dot{\theta}_1) + \tfrac{1}{2}m_2(\dot{X}^2 + 2\dot{X}L_1\dot{\theta}_1$$

$$+2\dot{X}L_2\dot{\theta}_2 + 2L_1L_2\dot{\theta}_1\dot{\theta}_2 + L_1^2\dot{\theta}_1^2 + L_2^2\dot{\theta}_2^2) - m_1gL_1$$

$$+ m_1gL_1\cos\theta_1 - m_2gL_1 + m_2gL_1\cos\theta_1 - m_2gL_2$$

$$+ m_2gL_2\cos\theta_2. \qquad (2\text{-}5)$$

2.6 Equations of Motion

The differential equations governing the motion of the system shown in Fig. (3) are obtained by substituting Eq. (2-5) into Eq. (2-1) with $q_1 = \theta_1$ and $q_2 = \theta_2$. The results after rearranging terms and assuming small angles are given as follows; i.e.,

$$(m_1L_1^2 + m_2L_1^2)\ddot{\theta}_1 + m_2L_1L_2\ddot{\theta}_2 + (m_1gL_1 + m_2gL_1)\theta_1 =$$

$$- (m_1L_1 + m_2L_1)\ddot{X}, \text{ and} \qquad (2\text{-}6)$$

$$(m_2L_1L_2)\ddot{\theta}_1 + (m_2L_2^2)\ddot{\theta}_2 + m_2gL_2\theta_2 = - m_2L_2\ddot{X}. \qquad (2\text{-}7)$$

Eqs. (2-6) and (2-7) are the differential equations governing the motion of the idealized balloon system. The equations of motion in the mutually perpendicular plane are the same, however $\theta_1 = \psi_1$ and $\theta_2 = \psi_2$, these equations can be written as:

$$(m_1L_1^2 + m_2L_1^2)\ddot{\psi}_1 + m_2L_1L_2\ddot{\psi}_2 + (m_1gL_1 + m_2gL_1)\psi_1 =$$

$$- (m_1L_1 + m_2L_1)\ddot{X}, \text{ and} \qquad (2\text{-}8)$$

$$(m_2 L_1 L_2)\ddot{\psi}_1 + (m_2 L_2^2)\ddot{\psi}_2 + m_2 g L_2 \psi_2 = -m_2 L_2 \ddot{x} \qquad (2\text{-}9)$$

One method of solving these equations will be discussed in the following chapter.

CHAPTER III

RESPONSE OF BALLOON BORN OBSERVATION PLATFORM

3.1 Development of Lumped Parameter Modal Equations

The method of modal analysis can be used to transform the simultaneous coupled differential equations of motion of a lumped system into a set of uncoupled differential equations, (Ref. 5). These resulting equations can easily be solved to obtain the response as a function of various initial conditions and excitations.

The mathematical model for any generally linear lumped parameter mechanical system without damping can be written in matrix form as follows; i.e.,

$$M\ddot{q} + Kq = F, \tag{3-1}$$

where

M = mass matrix,

K = stiffnes matrix,

q = vector of generalized coordinates, and

F = forcing function.

To use the method of modal analysis, it is necessay to solve the eigenvalue problem associated with the homogeneous system described by Eq. (3-1). The eigenvalue problem can be expressed as follows; i.e.,

$$\omega_i^2 M u_i = K u_i \tag{3-2}$$

where

$\omega_i^2 = i^{th}$ eigenvalue, and

$u_i = i^{th}$ eigenvector.

The eigenvectors can be normalized such that:

$$\tilde{u}_i^T M \tilde{u}_j = \delta_{ij}, \tag{3-3}$$

$$\tilde{u}_i^T K \tilde{u}_j = \omega_i^2 \delta_{ij}, \tag{3-4}$$

where

$\tilde{u}_i = i^{th}$ normalized eigenvector,

$\tilde{u}_j = j^{th}$ normalized eigenvector, and

δ_{ij} = Kronecker Delta.

$= 1 \quad i=j$

$= 0 \quad i \neq j$

It can be shown that:

$$\tilde{u}_i = C_i u_i, \tag{3-5}$$

where

$$C_i^2 = u_i^T M u_i. \tag{3-6}$$

The resulting modal matrix U is such that:

$$U^T M U = I, \tag{3-7}$$

and

$$U^T K U = \omega^2, \tag{3-8}$$

where

$$U = [\tilde{u}_1 \tilde{u}_2], \tag{3-9}$$

I = identity matrix, and

ω^2 = diagonal matrix of the eigenvalues.

The non-homogeneous solution of Eq. (3-1) can now be described as follows; i.e.,

$$q = U\eta, \tag{3-10}$$

where

η = column matrix consisting of a set of time dependent generalized coordinates, and

q = column matrix of generalized displacements.

Substitution of Eq. (3-10) into Eq. (3-1) yields;

$$MU\ddot{\eta} + KU\eta = F. \tag{3-11}$$

Premultiplying both sides of Eq. (3-11) by U^T yields the following; i.e.,

$$U^T M U\ddot{\eta} + U^T K U\eta = U^T F \tag{3-12}$$

Introduction of Eqs. (3-7) and (3-8) into Eq. (3-12) gives the following expression; i.e.,

$$\ddot{\eta} + \omega^2 \eta = N, \tag{3-13}$$

where

$$N = U^T F. \tag{3-14}$$

Eq. (3-13) represents a set of n uncoupled differential equations of the form:

$$\ddot{\eta}_i(t) + \omega_i^2 \eta_i(t) = N_i \qquad i = 1,2,\ldots,n. \tag{3-15}$$

These equations have the form of the differential equations describing the motion of n, undamped, uncoupled single degree of freedom systems.

Eq. (3-15) can be solved by means of the Laplace transform method, this yields:

$$\eta_i(t) = \frac{1}{\omega_i}\int_0^t N_i(\tau)\sin\omega_i(t-\tau)d\tau + \eta_i(0)\cos\omega_i t + \eta_i(0)\frac{\sin\omega_i t}{\omega_i} \qquad i = 1,2,\ldots,n. \tag{3-16}$$

Assuming zero initial conditions, Eq. (3-16) can be written as follows; i.e.,

$$\eta_i(t) = \frac{1}{\omega_i}\int_0^t N_i(\tau)\sin\omega_i(t-\tau)d\tau. \tag{3-17}$$

This equation is known as the convolution integral. The response q can be determined by introducing Eq. (3-17) into Eq. (3-10)

3.2 Response of Idealized Balloon System

The Eqs. (2-6),(2-7),(2-8), and (2-9) for the system shown in Fig. (3) can be written as follows:

$$\begin{bmatrix} m_1l_1^2+m_2l_1^2 & m_2l_1l_2 \\ m_2l_1l_2 & m_2l_2^2 \end{bmatrix} \begin{vmatrix} \ddot{q}_1 \\ \ddot{q}_2 \end{vmatrix} + \begin{bmatrix} m_1gl_1+m_2gl_1 & 0 \\ 0 & m_2gl_2 \end{bmatrix} \begin{vmatrix} q_2 \\ q_2 \end{vmatrix}$$

$$= \begin{vmatrix} -(m_1l_1+m_2l_1)\ddot{x} \\ -(m_2l_2)\ddot{x} \end{vmatrix}, \qquad (3\text{-}18)$$

or in abbreviated form as:

$$Mq + Kq = F, \qquad (3\text{-}19)$$

where

$$M = \begin{bmatrix} m_{11} & m_{12} \\ m_{21} & m_{22} \end{bmatrix},$$

$$K = \begin{bmatrix} k_{11} & 0 \\ 0 & k_{22} \end{bmatrix}, \text{and}$$

$$F = \begin{vmatrix} -(m_1l_1+m_2l_1)\ddot{x} \\ -(m_2l_2)\ddot{x} \end{vmatrix}.$$

A non trivial solution of the eigenvalue problem given by Eq. (3-2) will result if and only if the determinant of the coefficients vanish; i.e.,

$$|K - \omega^2 M| = 0. \qquad (3\text{-}20)$$

Introduction of the proper elements of Eq. (3-19) into Eq. (3-20) yields.

$$\begin{vmatrix} k_{11} - m_1\omega^2 & -m_{12}\omega^2 \\ -m_{21}\omega^2 & k_{22} - m_{22}\omega^2 \end{vmatrix} = 0. \qquad (3\text{-}21)$$

Solving Eq. (3-21) for ω^2 results in two real roots given by the expression:

$$\omega_i^2 = 1/2\frac{(k_{11}m_{11}+k_{22}m_{11})}{(m_{11}m_{22}-m_{12}m_{21})} \pm 1/2\sqrt{\frac{(k_{11}m_{22}+k_{22}m_{11})^2}{(m_{11}m_{22}-m_{12}m_{21})^2} - \frac{4k_{11}k_{22}}{(m_{11}m_{22}-m_{12}m_{21}}}, \qquad (3\text{-}22)$$

where

ω_i = natural frequency, and

$i = 1,2.$

The eigenvectors associated with each natural frequency can now be written as; i.e.,

$$u_1 = \begin{vmatrix} 1 \\ \dfrac{k_{11} - \omega_1^2 m_{11}}{\omega_1^2 m_{12}} \end{vmatrix}, \qquad (3\text{-}23)$$

and

$$u_2 = \begin{vmatrix} 1 \\ \dfrac{k_{11} - \omega_2^2 m_{11}}{\omega_2^2 m_{12}} \end{vmatrix}, \qquad (3\text{-}24)$$

where

u_1 = eigenvector associated with ω_1, and

u_2 = eigenvector associated with ω_2.

The characteristic vectors u_1 and u_2 are the modal vectors and represent the natural modes of oscillation of the system. Normalization of the modal vectors will produce the normal modes. Computing the values of C_1 and C_2 according to Eq. (3-6) yields the following:

$$C_1 = \sqrt{m_{11} + \frac{(k_{11} - \omega_1^2 m_{11})}{\omega_1^2 m_{12}}(m_{21} + m_{12}) + \frac{(k_{11} - \omega_1^2 m_{11})^2}{(\omega_1^2 m_{12})^2} m_{22}}, \qquad (3\text{-}25)$$

$$C_2 = \sqrt{m_{11} + \frac{(k_{11} - \omega_2^2 m_{11})}{\omega_2^2 m_{12}}(m_{21} + m_{12}) + \frac{(k_{11} - \omega_2^2 m_{11})^2}{(\omega_2^2 m_{12})^2} m_{22}}. \qquad (3\text{-}26)$$

The resulting normalized modal vectors become:

$$\tilde{u}_1 = \begin{vmatrix} 1 \\ \dfrac{k_{11} - \omega_1^2 m_{11}}{\omega_1^2 m_{12}} \end{vmatrix}, \text{ and} \qquad (3\text{-}27)$$

$$\tilde{u}_1 = \begin{vmatrix} 1 \\ \dfrac{k_{11} - \omega_2^2 m_{11}}{\omega_2^2 m_{12}} \end{vmatrix}. \qquad (3\text{-}28)$$

Substituting Eqs. (3-27) and (3-28) into Eq. (3-9) yields the modal matrix U; i.e.,

$$U = \begin{bmatrix} \dfrac{1}{C_1} & \dfrac{1}{C_2} \\ \dfrac{k_{11} - \omega_1^2 m_{11}}{C_1 \omega_1^2 m_{12}} & \dfrac{k_{11} - \omega_2^2 m_{11}}{C_2 \omega_2^2 m_{12}} \end{bmatrix} \qquad (3\text{-}29)$$

Substitution of the modal matrix U given by Eq. (3-29) into Eq. (3-14) yields the following for the components of vector N; i.e.,

$$N_1 = -(m_1 l_1 + m_2 l_2)\ddot{x}u_{11} - (m_2 l_2)\ddot{x}u_{21}, \text{ and}$$

$$N_2 = -(m_1 l_1 + m_2 l_2)\ddot{x}u_{12} - (m_2 l_2)\ddot{x}u_{22},$$

where

u_{ij} = components of modal matrix U.

Introducing the the above components into Eq. (3-17) yields the following set of expressions; i.e.,

$$\eta_1(t) = \frac{1}{\omega_1}\int_0^t N_1(\tau)\sin\omega_1(t-\tau)d\tau, \text{ and} \tag{3-30}$$

$$\eta_2(t) = \frac{1}{\omega_2}\int_0^t N_2(\tau)\sin\omega_2(t-\tau)d\tau. \tag{3-31}$$

The system response given by Eq. (3-10) can now be written as follows:

$$q_1 = \eta_1(t)u_{11} + \eta_2(t)u_{12}, \text{ and} \tag{3-32}$$

$$q_2 = \eta_1(t)u_{21} + \eta_2(t)u_{22}. \tag{3-33}$$

The next chapter will discuss the numerical evaluation of q_1 and q_2 in order to obtain the response of the system shown in Fig. (3).

CHAPTER IV

RESULTS AND SUMMARY

4.1 LACATE Mission Data

Fig. (1) illustrates the actual LACATE balloon system and Fig. (3) illustrates the system as it was idealized for this study. The physical properties of the idealized LACATE system are given in Table I. The results of the eigenvalue problem from Eq. (3-2) are presented in Table II. The resulting natural frequencies, periods, and mode shapes are given in Table III.

4.2 Balloon System Horizontal Accelerations

The flight of the LACATE balloon system was tracked by ground radar and the resulting horizontal trajectory is shown in Fig. (4). Two typical segments of the balloon's flight path were analyzed in this study. Flight segment one is taken from the time interval $0 \leq t \leq 500$ seconds, while flight segment two is taken from the time interval $5889 \leq t \leq 6389$ seconds.

The hoizontal acceleration components a_1 and a_2 along the balloon's body axis were computed using data from the radar tracking station in conjunction with a numerical differentiation process, (Ref. 4). Figs. (5) and (6) show the body axis acceleration components a_1 and a_2 for the two flight segments studied.

4.3 Response of Balloon Borne Observation Platform

The values of η_1 and η_2 from Eqs. (3-30) and (3-31)

were determined by numerical integration of the convolution integral using a trapezoidal rule. (Refer to Appendix I for a listing of the computer program.) Fig. (7)-(14) give the response of η_1 and η_2 (with inputs a_1 and a_2) for each flight segment studied.

In order to verify the results of the computer program, the input a_1, from flight segment one was approximated as a straight line function for the interval $0 \leq t \leq 200$ seconds. The resulting approximation is shown in Fig. (15). Eq. (3-30) was then integrated analytically with this straight line approximation as input for $\ddot{x}$. The results are shown plotted in Fig. (16). Eq. (3-30) was also integrated numerically on the computer with the straight line function as input for $\ddot{x}$. (Refer to Appendix II for a listing of the computer program.) The results are given in Fig. (17).

The results from Eqs. (3-32) and (3-33) for θ_1, θ_2, ψ_1, and ψ_2 for flight segment one are presented in Figs. (18)-(23). Figs. (20) and (23, show the comparision of θ_1, θ_2, and ψ_1, ψ_2 respectively. The system response θ_1, θ_2, ψ_1, and ψ_2 for flight segment two are presented in Figs. (24)-(29).

4.4 Discussion of Results

The results in Fig. (4) indicate dramatically the presents of wind gusts during the flight of the LACATE balloon system. These gusts were sufficient to cause significant changes in the direction of the balloon's

flight path. Moreover, Figs. (5) and (6) indicate that because of the wind gusts the magnitude of the acceleration a_1 and a_2 varied from -0.123 m/sec^2 to 0.095m/sec^2 in flight segment one and -0.055m/sec^2 to 0.10m/sec^2 in flight segment two.

Figs. (16) and (17) indicate that the results η_1 and η_2 obtained from the computer program are in close agreement with the results obtained from the analytic method. This fact enables one to have confidence in the computer program and in the numerical integration algorithm. Figs. (7)-(15) show that the response of η_1 and η_2 is oscillatory in nature. Moreover, the relative magnitude of the oscillation increases or decreases as the input acceleration a_1 and a_2 increases or decreases.

The results in Figs. (20) and (26) indicate that the magnitudes of θ_1 and θ_2 are approximately equal. This is also true for ψ_1 and ψ_2 shown in Figs. (23) and (29). Figs. (30)-(33) show that the period of oscillation is approximately 10 seconds. These facts indicate that the idealized balloon system oscillates primarily in the most fundamental mode.

The results in Figs. (18)-(29) indicate that the system does not oscillate about its vertical axis. These figures show that the relative offset of oscillation is negative when the input is postive and vice versa. The figures indicate also, that the relative swing amplitude increases and decreases as the input acceleration increases

and decreases.

4.5 Summary

In this study the balloon borne observation platform was viewed as a double pendulum with a moving (accelerating) support. The acceleration of the support which is due to the effect of wind gusts acting on the balloon was treated as an idealized source.

The results of this study indicate that the system oscillates primarily in the most fundamental mode. This is significant because, the balloon system can therefore be treated as a single pendulum with a moving (accelerating) support. This will simplify the mathermatical model in future idealizations. The results of this study also indicate, that due to the effect of wind gusts the maximum pendulation angle is of the order 1.0 degree. Generally these angles were found to be of the order 0.60 degrees or less. This is important to designers of future balloon systems inorder for them to determine what kinds of auxillary controls and or atitude determination systems are necessary for economical and accurate data collection.

TABLE I

Idealized LACATE System Properties

l_1 = 75ft (distance from support point O to mass m_1)

l_2 = 15ft (distance from mass m_1 to mass m_2)

m_1 = 135lb_m (lumped mass)

m_2 = 375lb_m (lumped mass)

TABLE II

Balloon System Eigenvalues, Natural Frequencies, and Corresponding Eigenvectors

i	ω_i^2	ω_i	u_i
1	0.3718	0.6098	1.000 1.044
2	9.3782	3.0624	1.000 -6.489

TABLE III

Natural Frequencies, Periods, and

Modal Shapes for Balloon System

i	ω_i	Period τ_i	Modal Shape
1	0.6098	10.303 sec	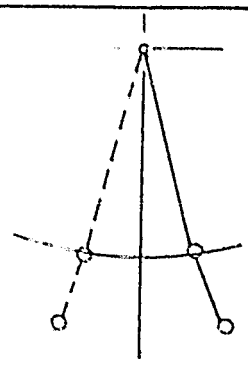
2	3.0624	2.051 sec	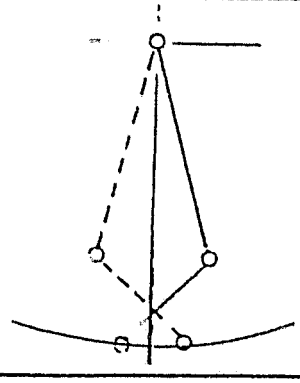

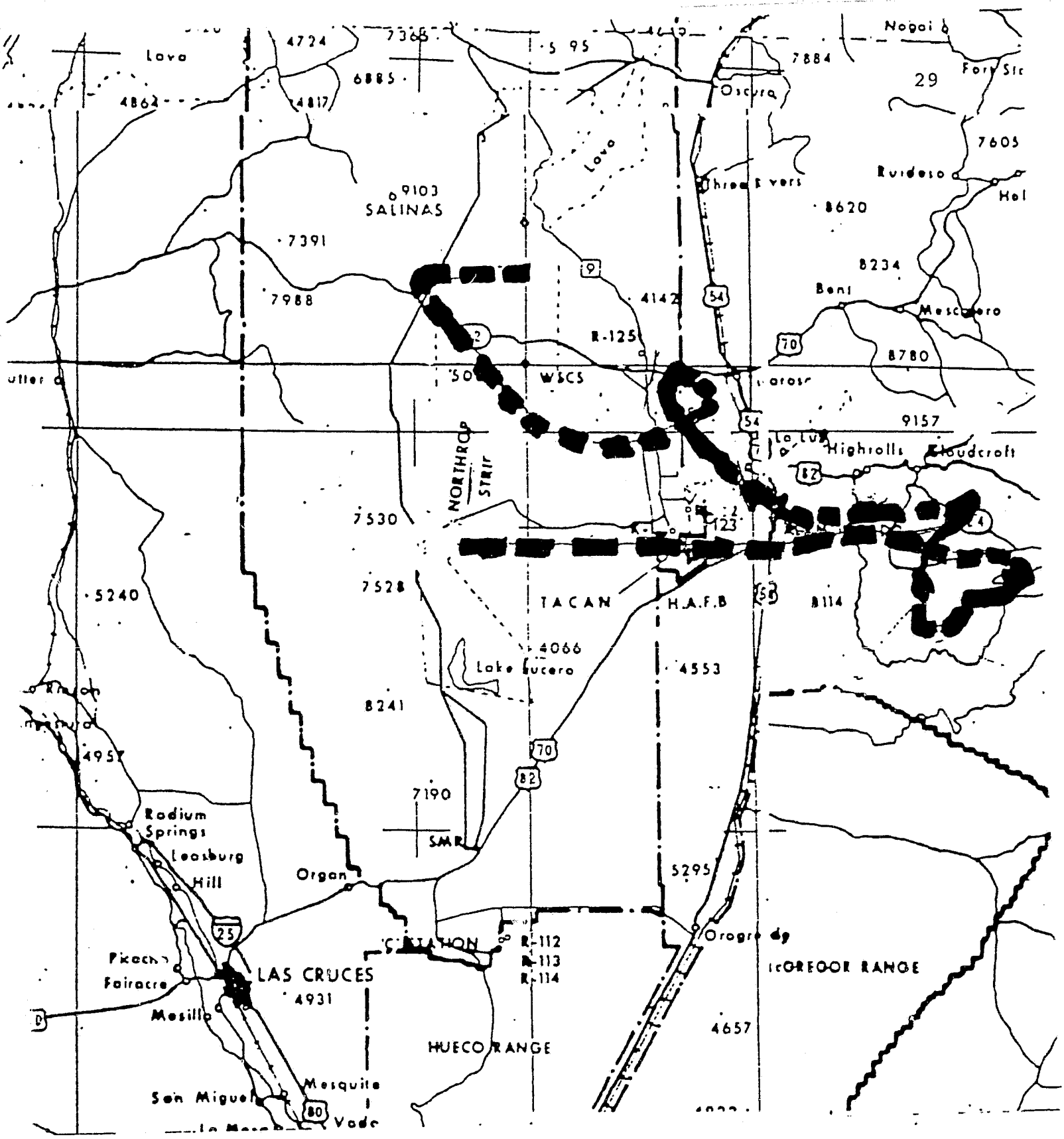

Figure (4) Balloon System Flight Path

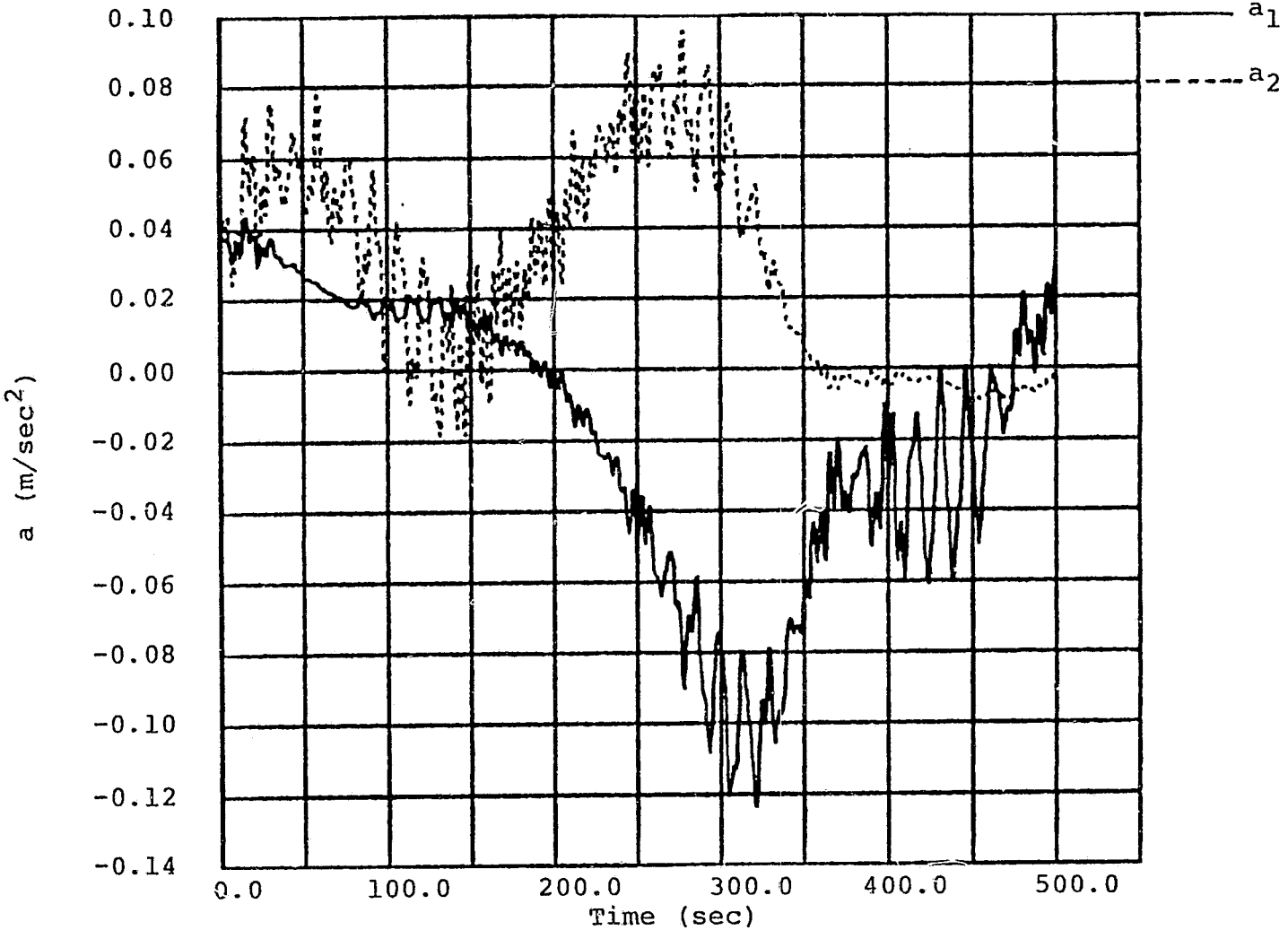

Figure (5) Horizontal Acceleration of Support Point O Along Body Axis (Flight Segment One)

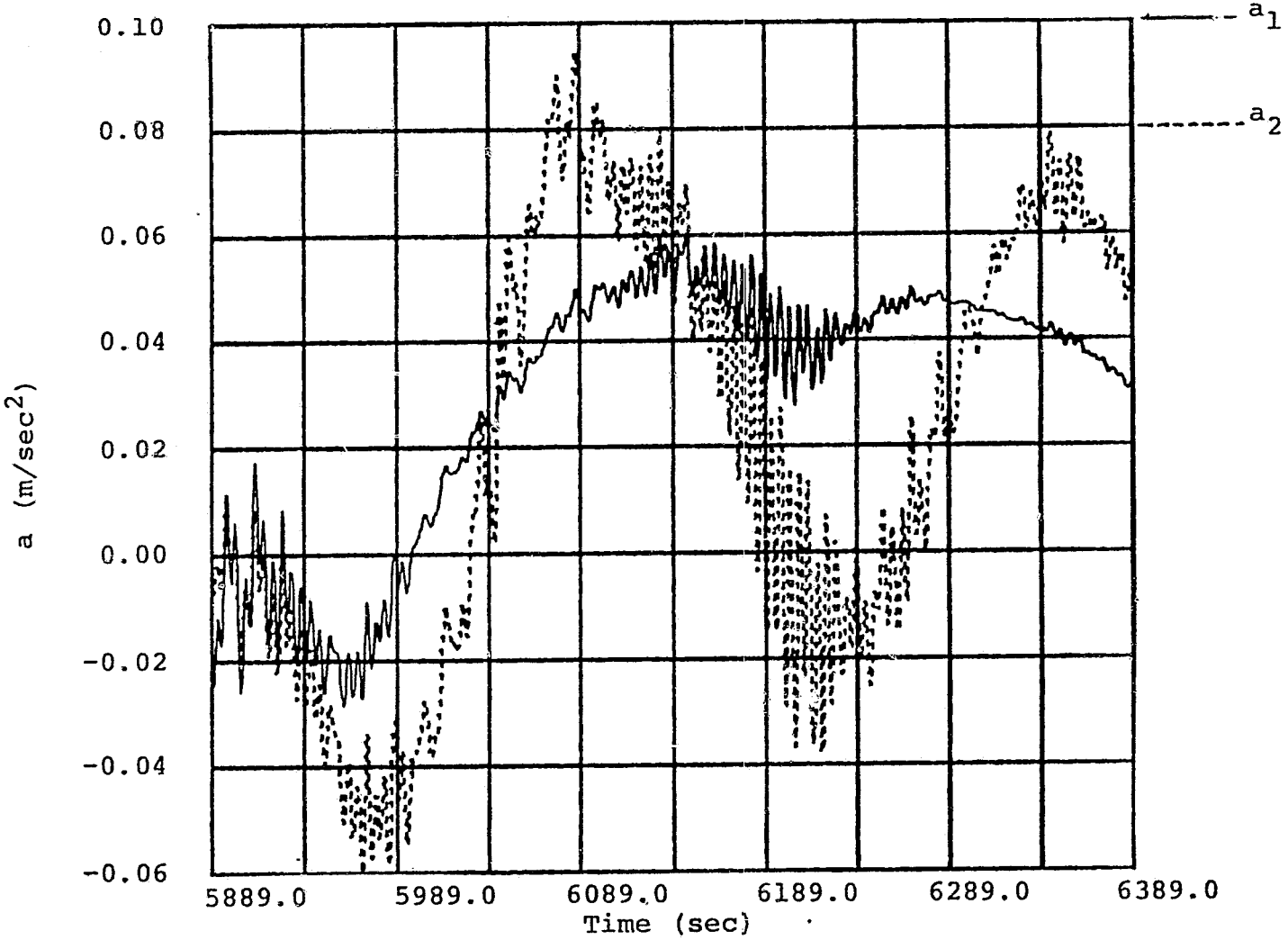

Figure (6) Horizontal Acceleration of Support Point O Along Body Axis (Flight Segment Two)

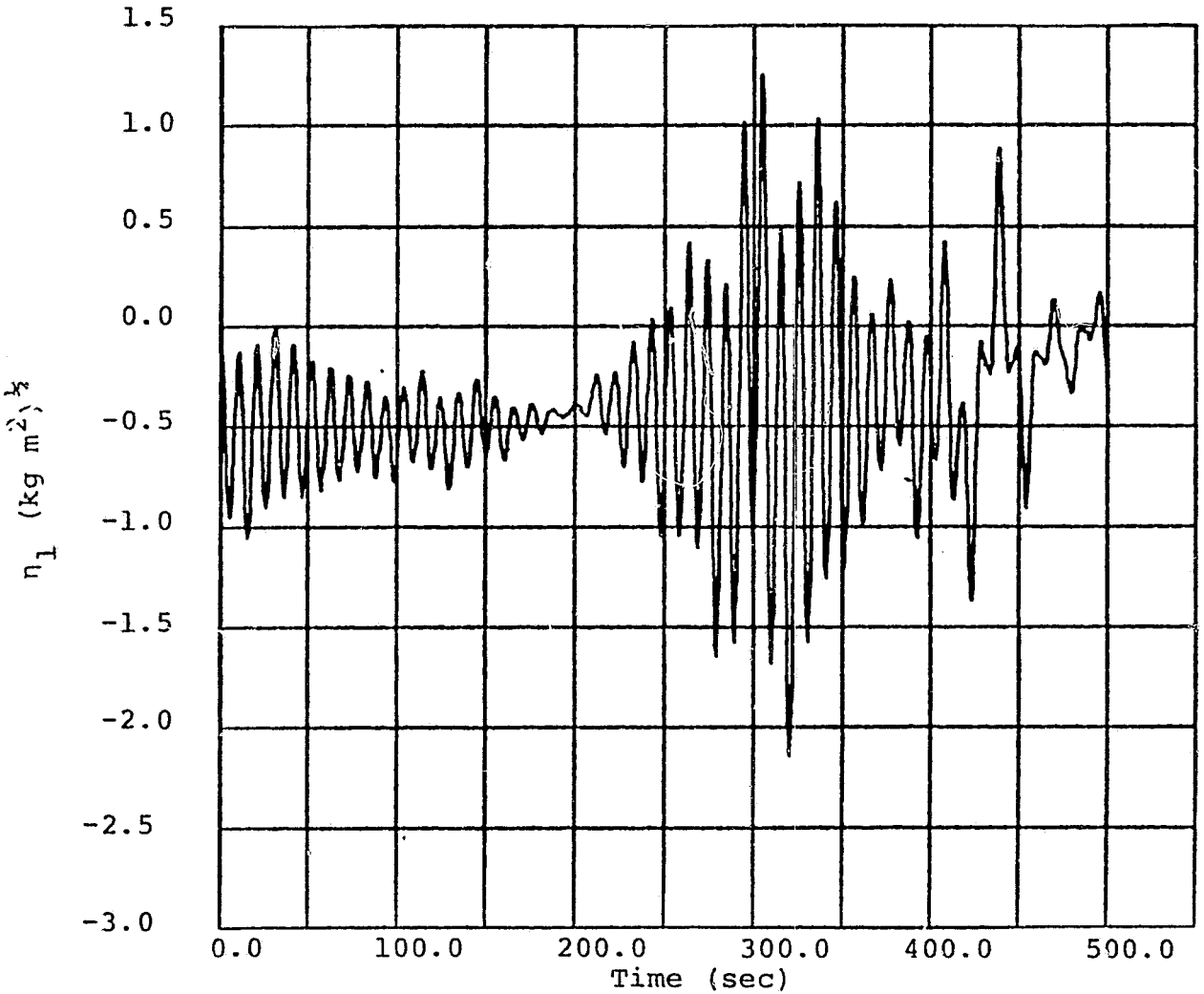

Figure (7) Plot of η_1 Values (With Input = a_1)

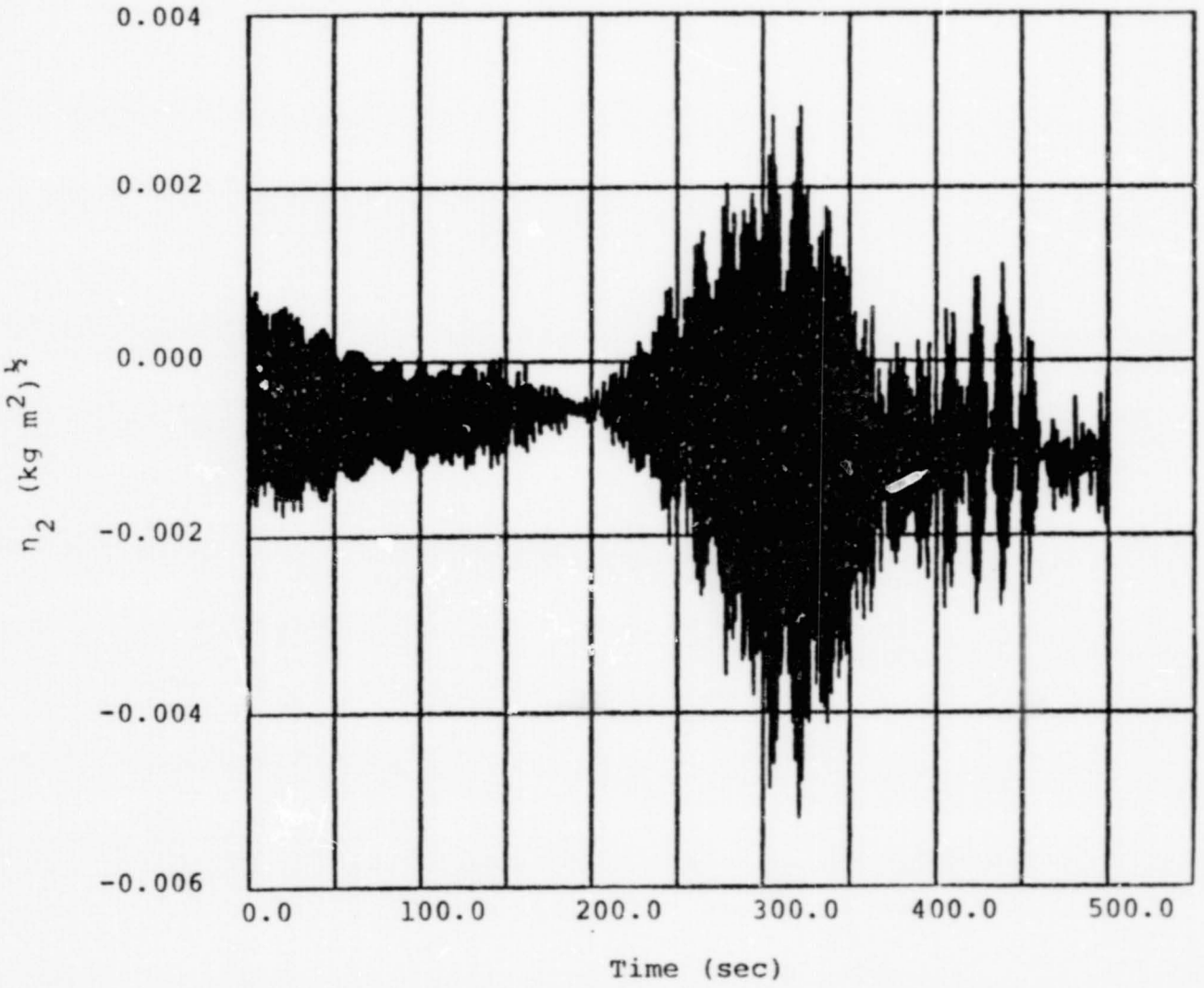

Figure (8) Plot of η_2 Values (With Input a_1)

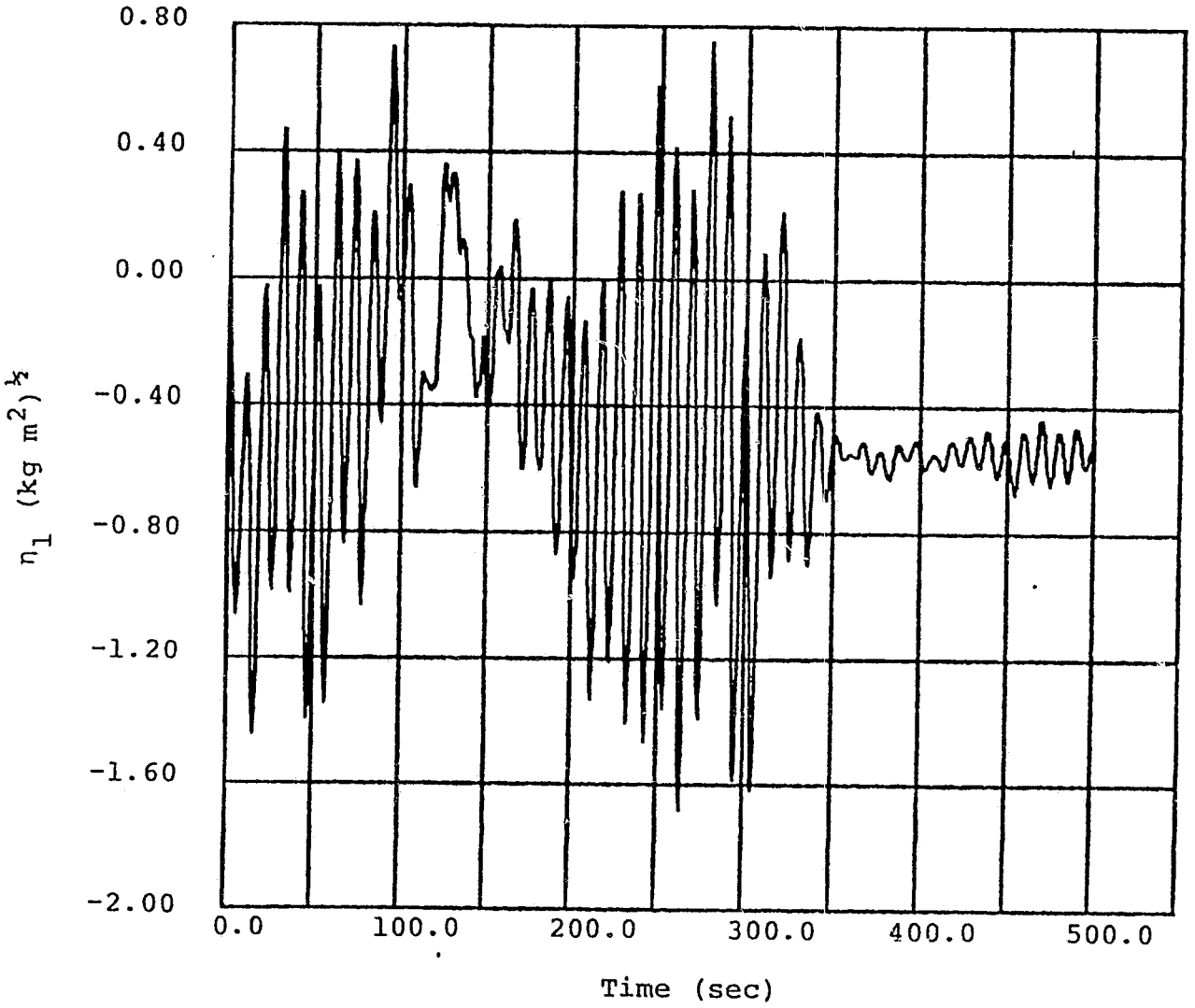

Figure (9) Plot of η_1 Values (With Input = a_2)

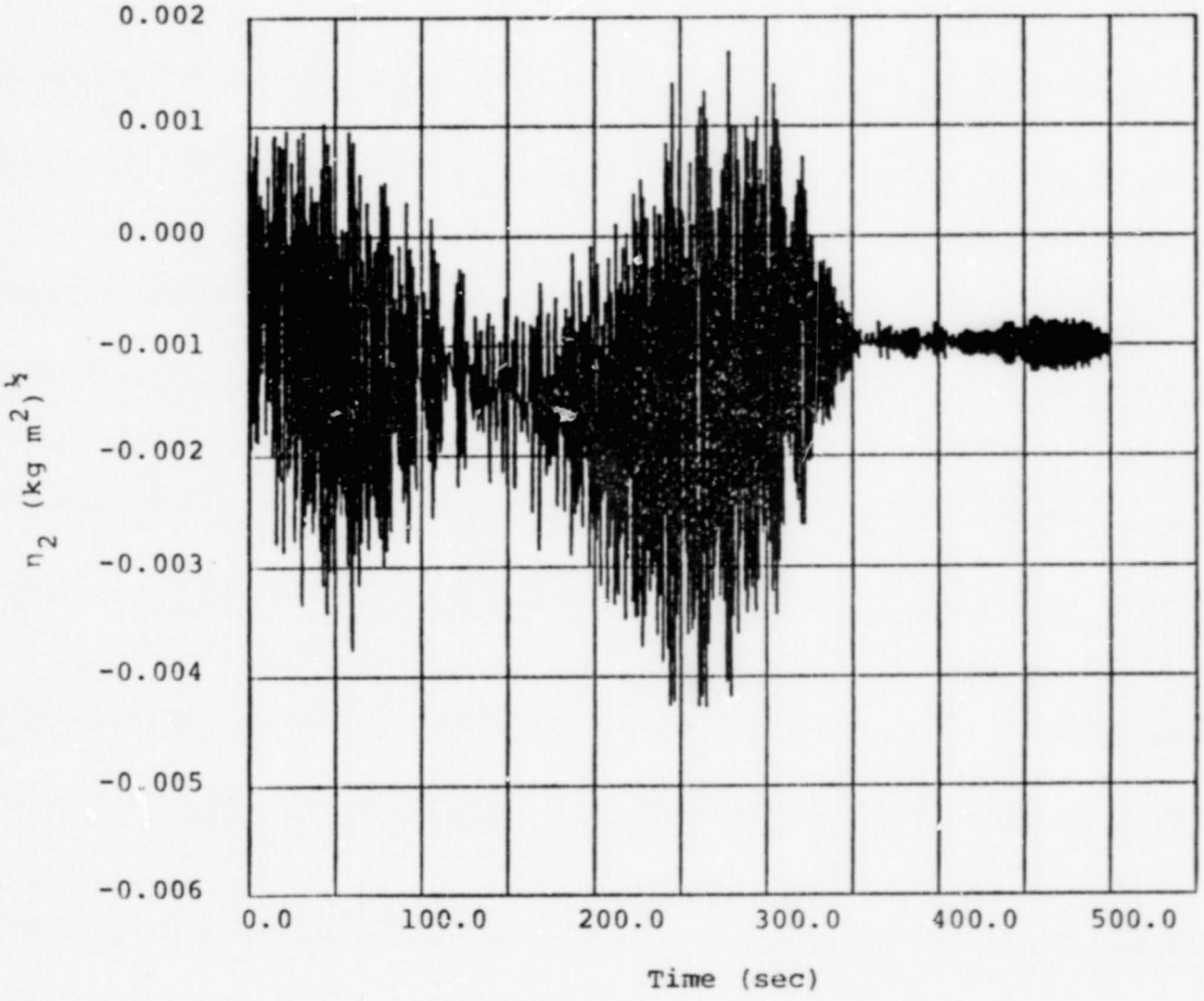

Figure (10) Plot of η_2 Values (With Input = a_2)

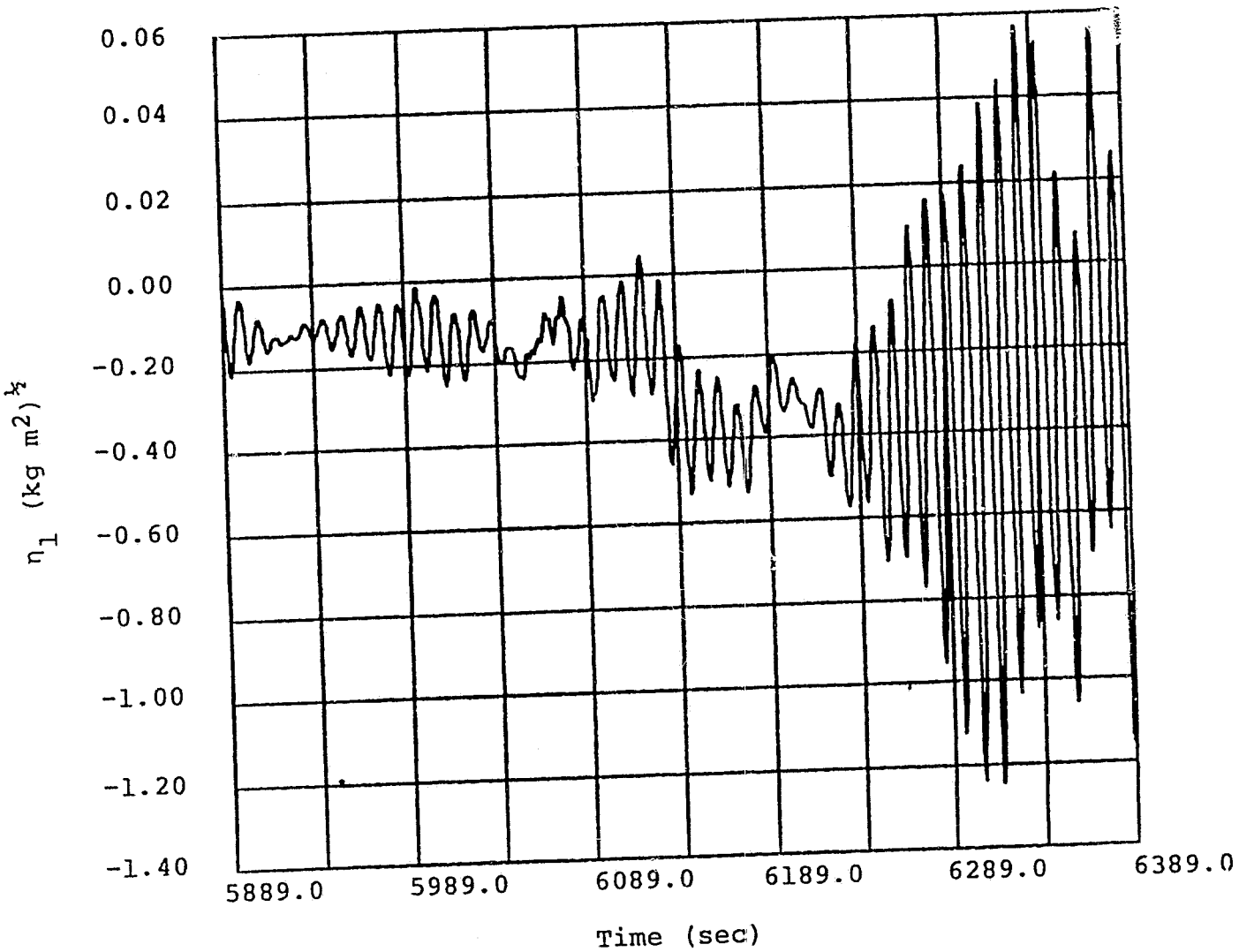

Figure (11) Plot of η_1 Values (With Input = a_1)

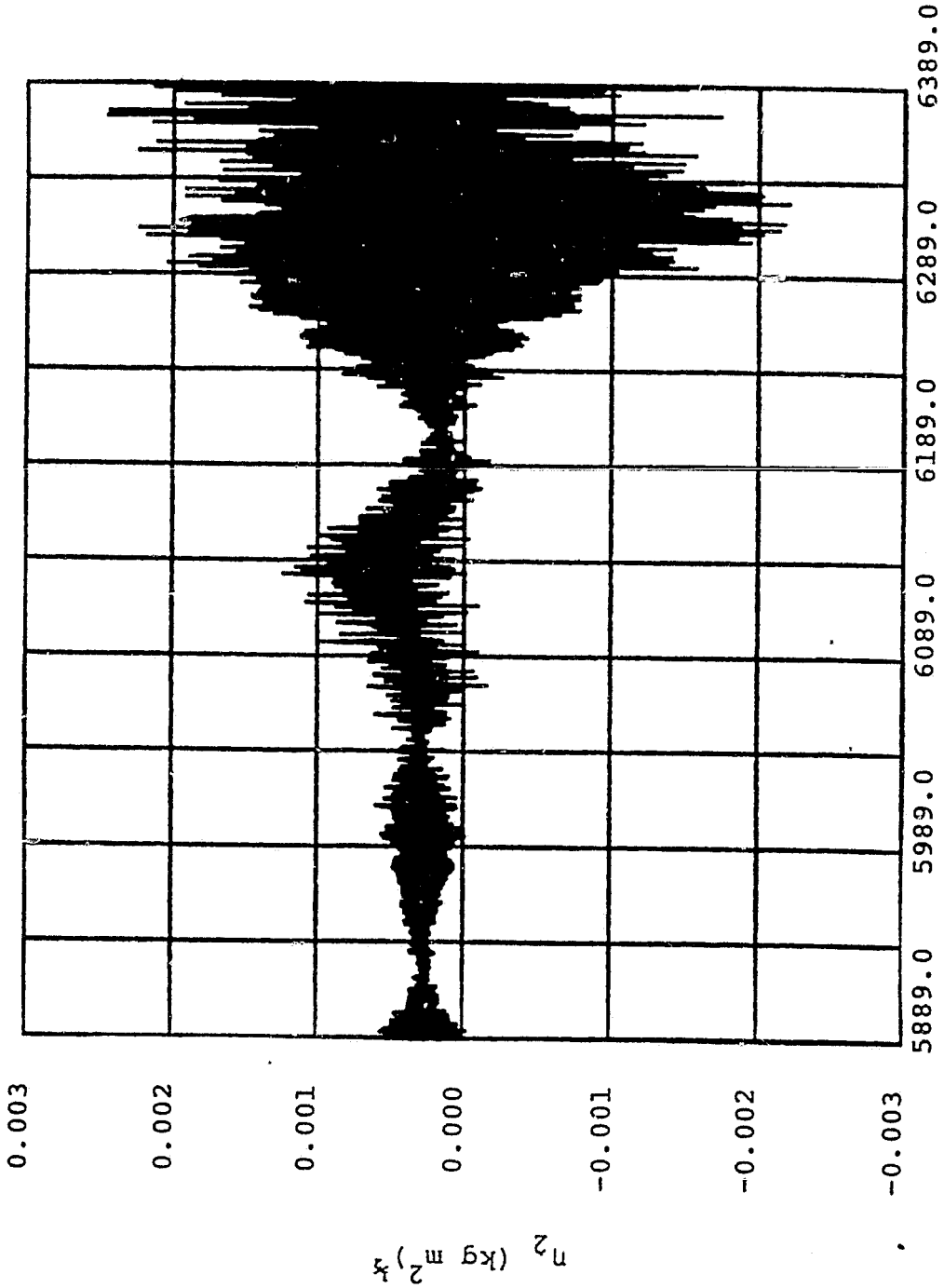

Figure (12) Plot of η_2 Values (With Input = a_1)

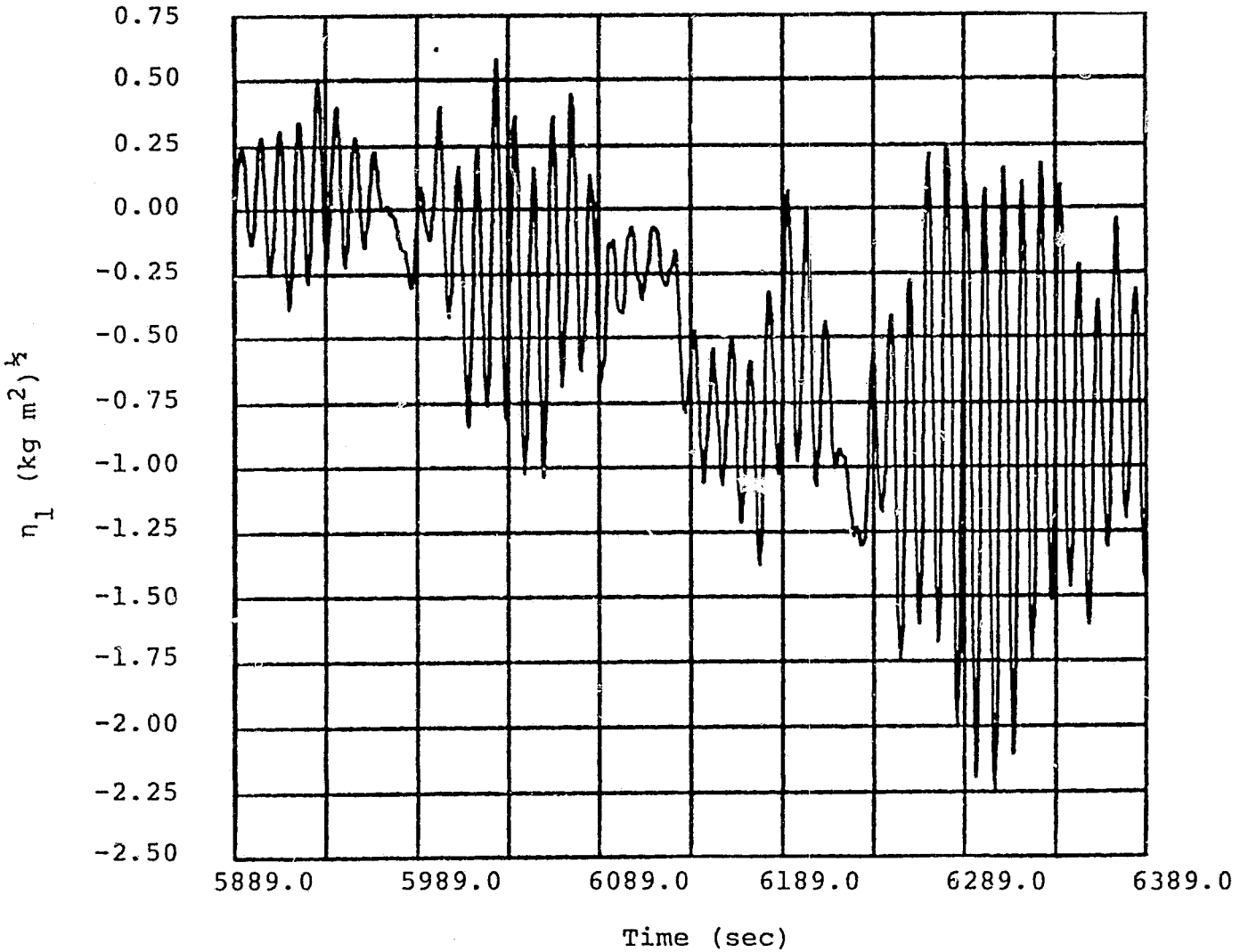

Figure (13) Plot of η_1 Values (With Input = a_2)

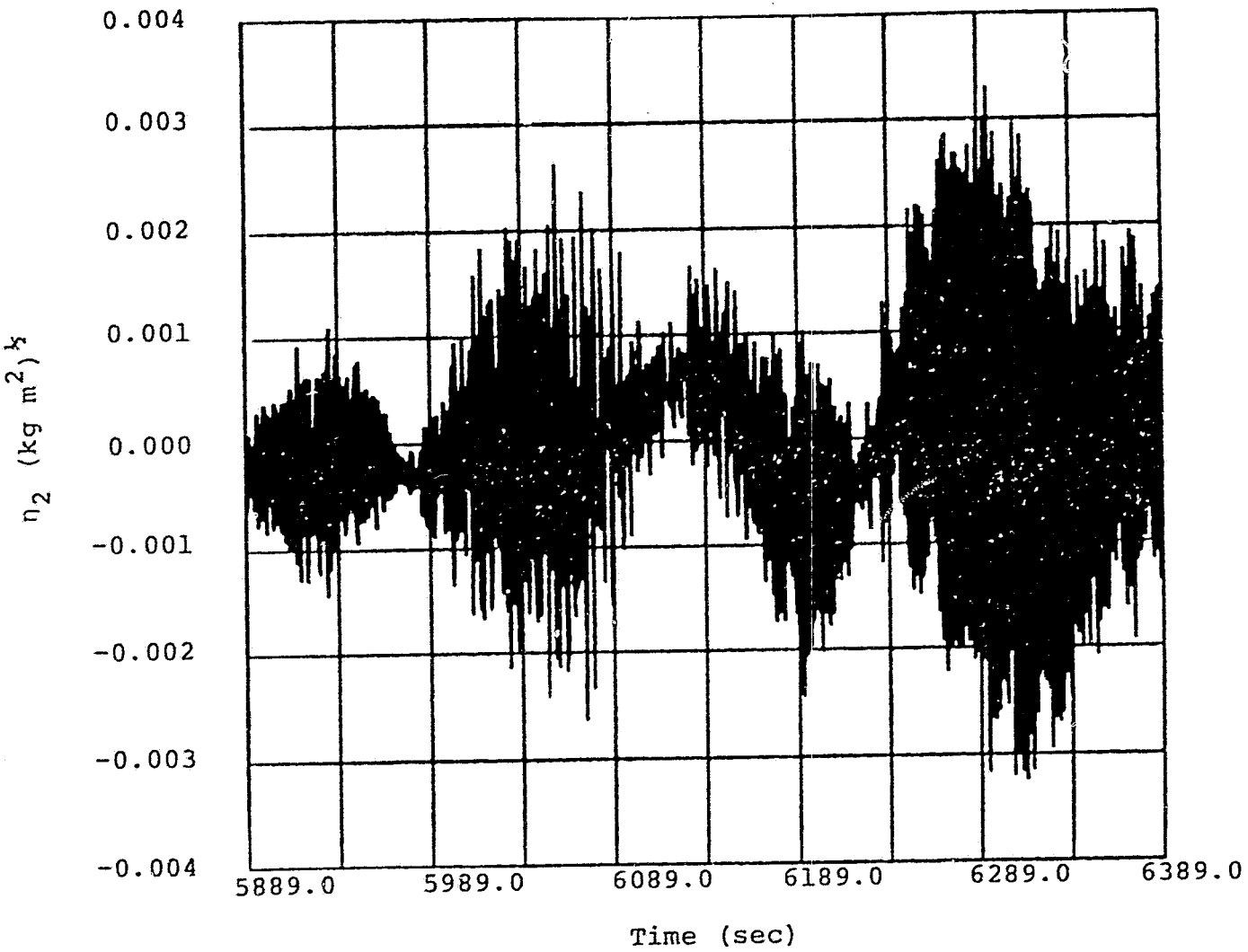

Figure (14) Plot of η_2 Values (With Input = a_2)

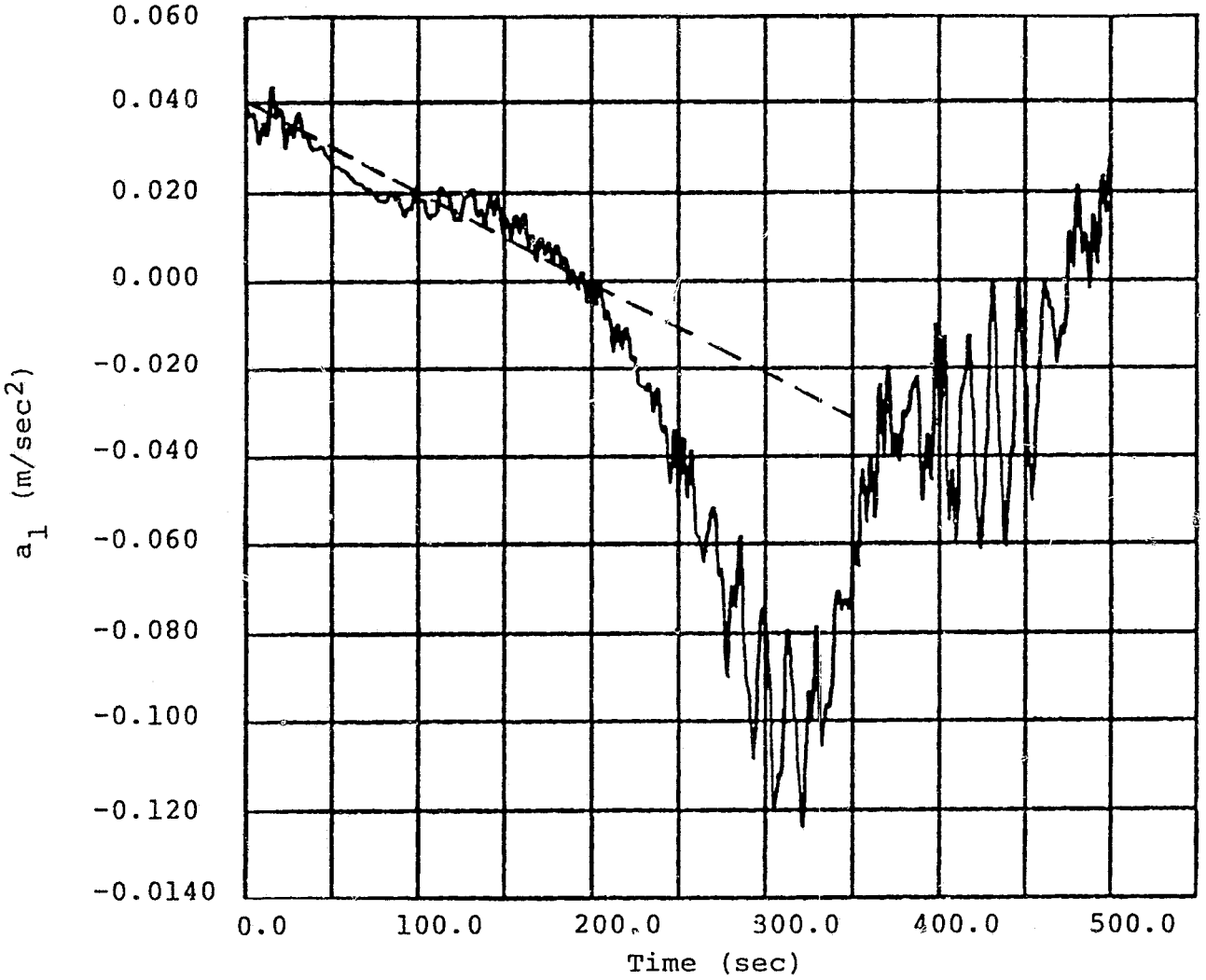

Figure (15) Plot of Straight Line Approximation
Flight Segment One

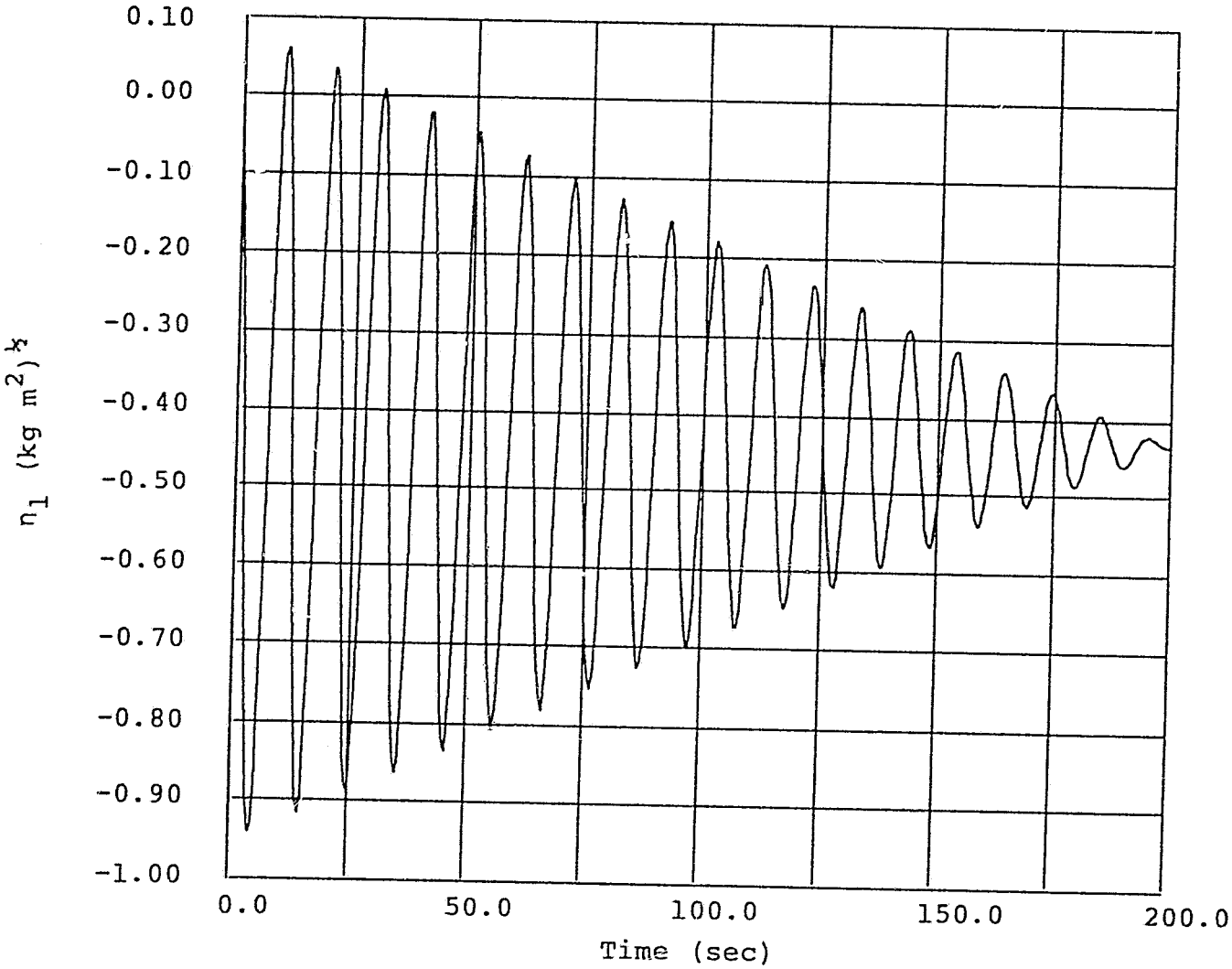

Figure (16) η_1 Values Computed Analytically (With Input = Straight Line Function)

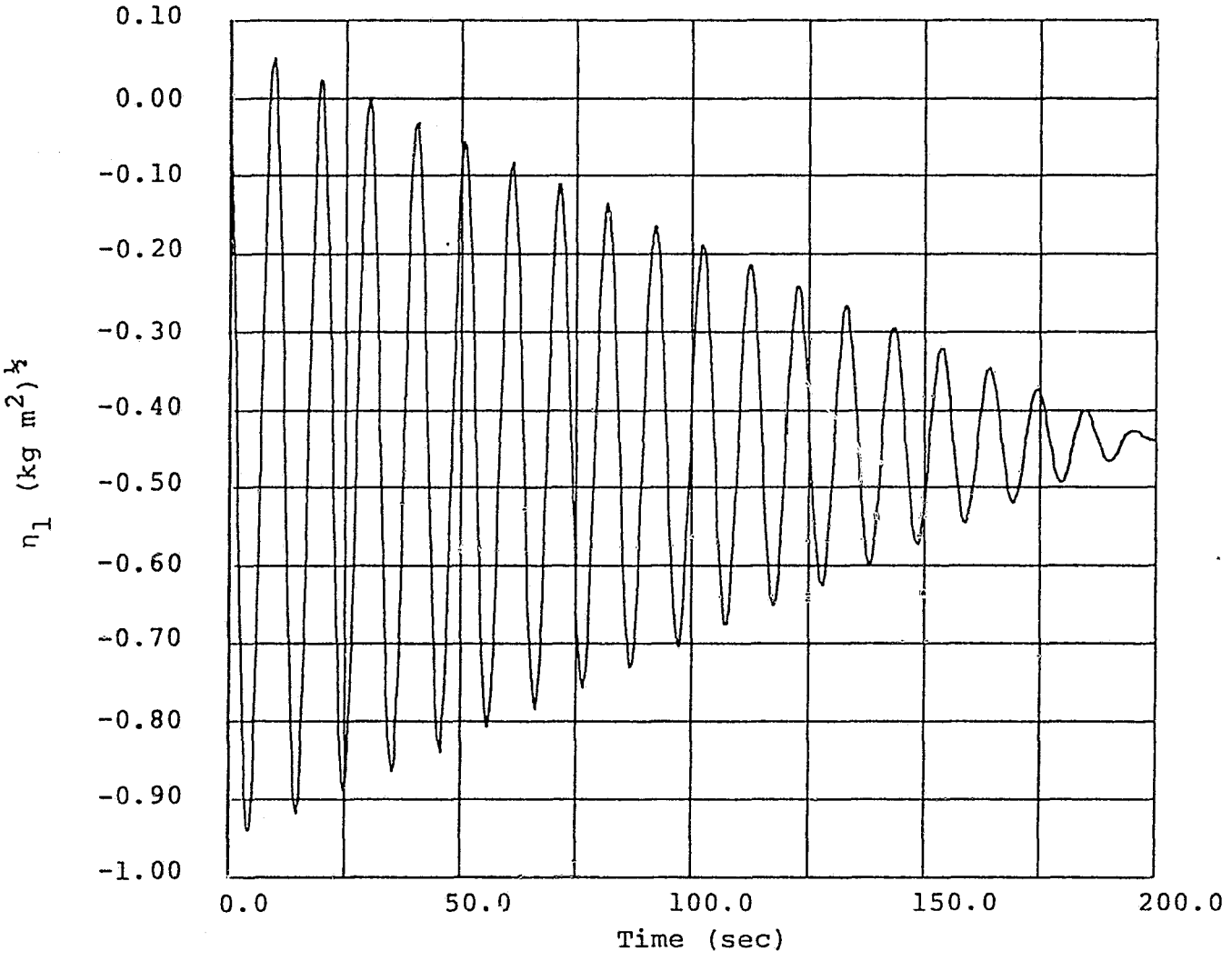

Figure (17) η_1 Values Computed Numerically (With Input = Straight Line Function)

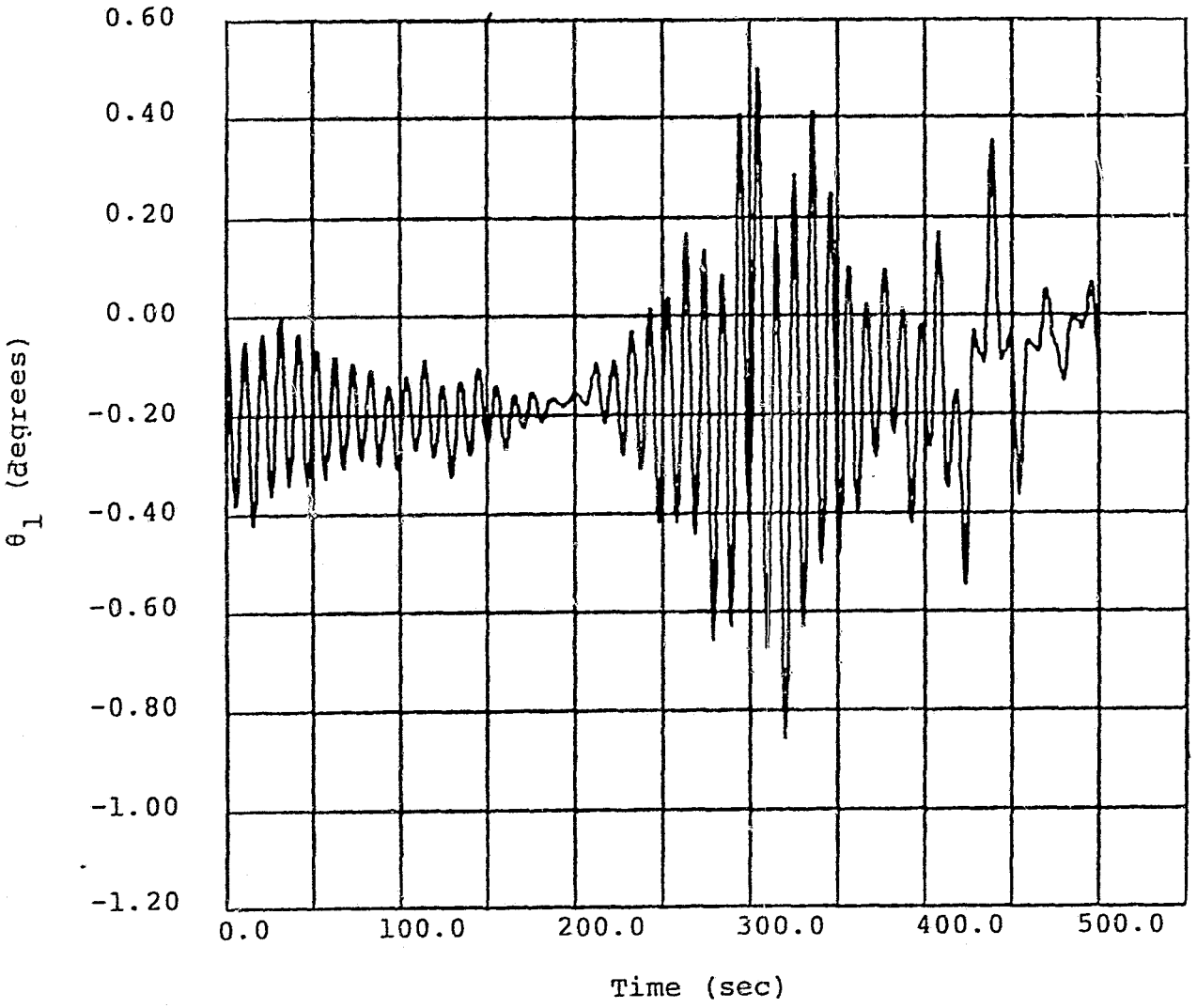

Figure (18) System Response (With Input = a_1)

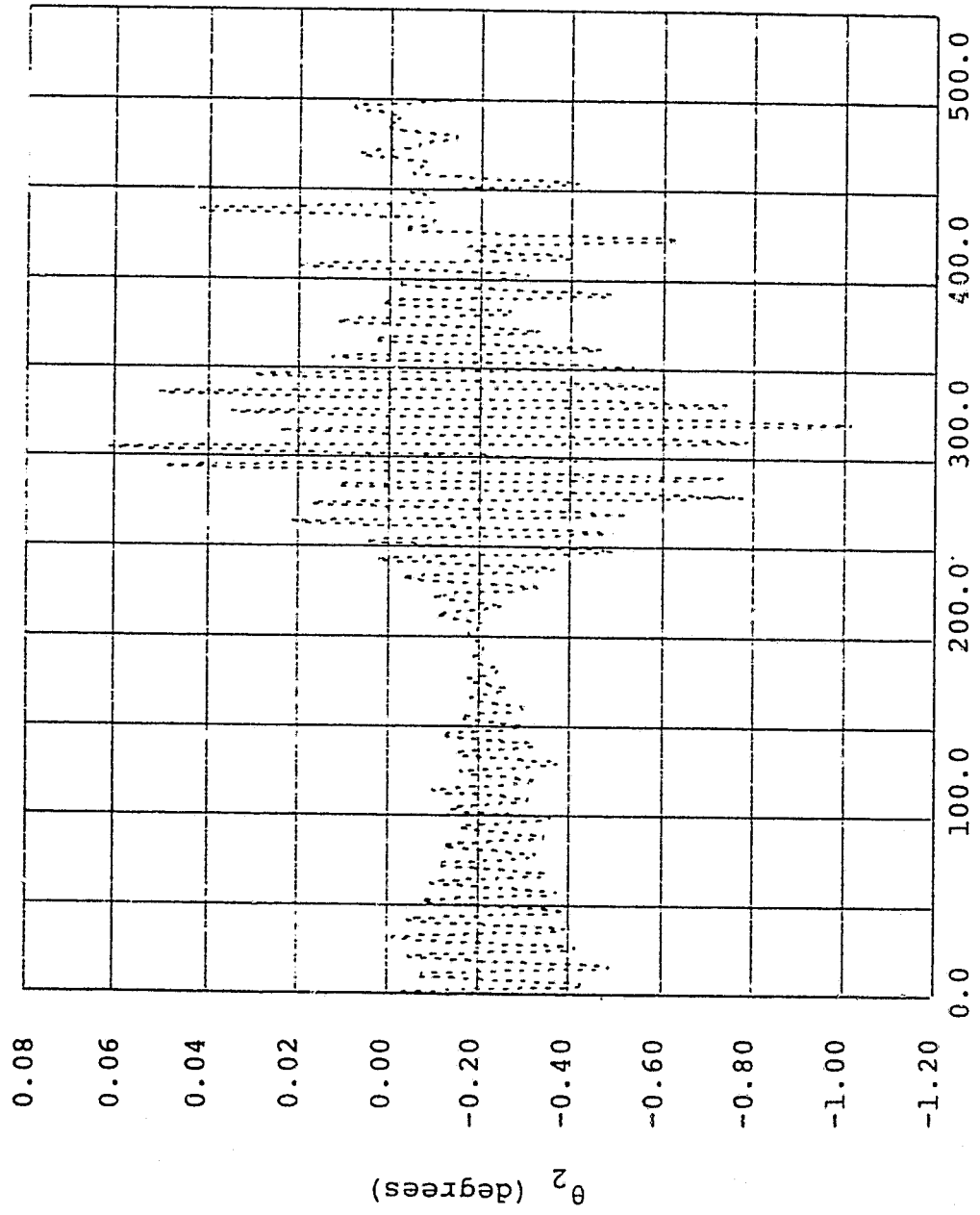

Figure (19) System Response (With Input = a_1)

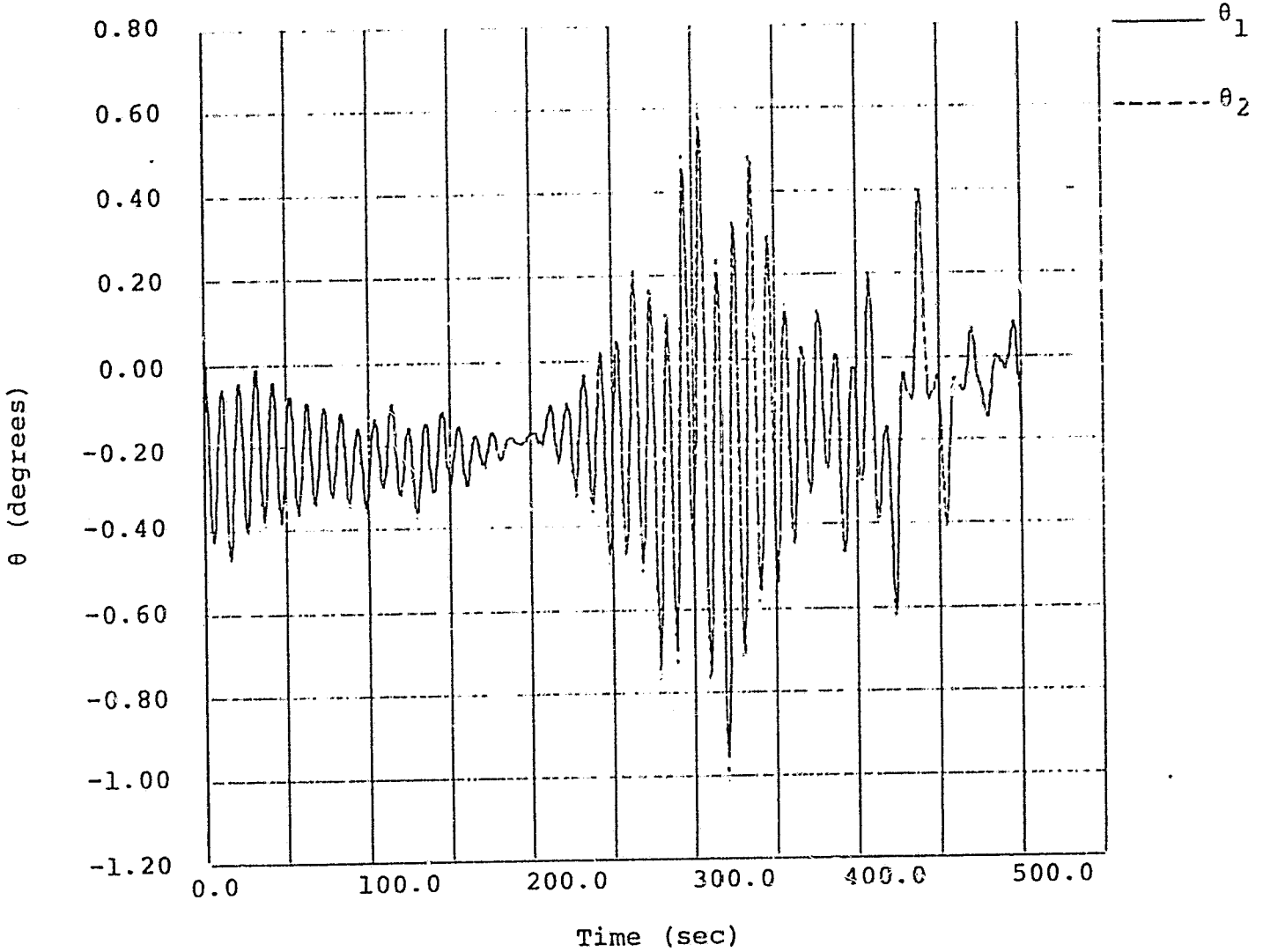

Figure (20) System Response (With Input = a_1)

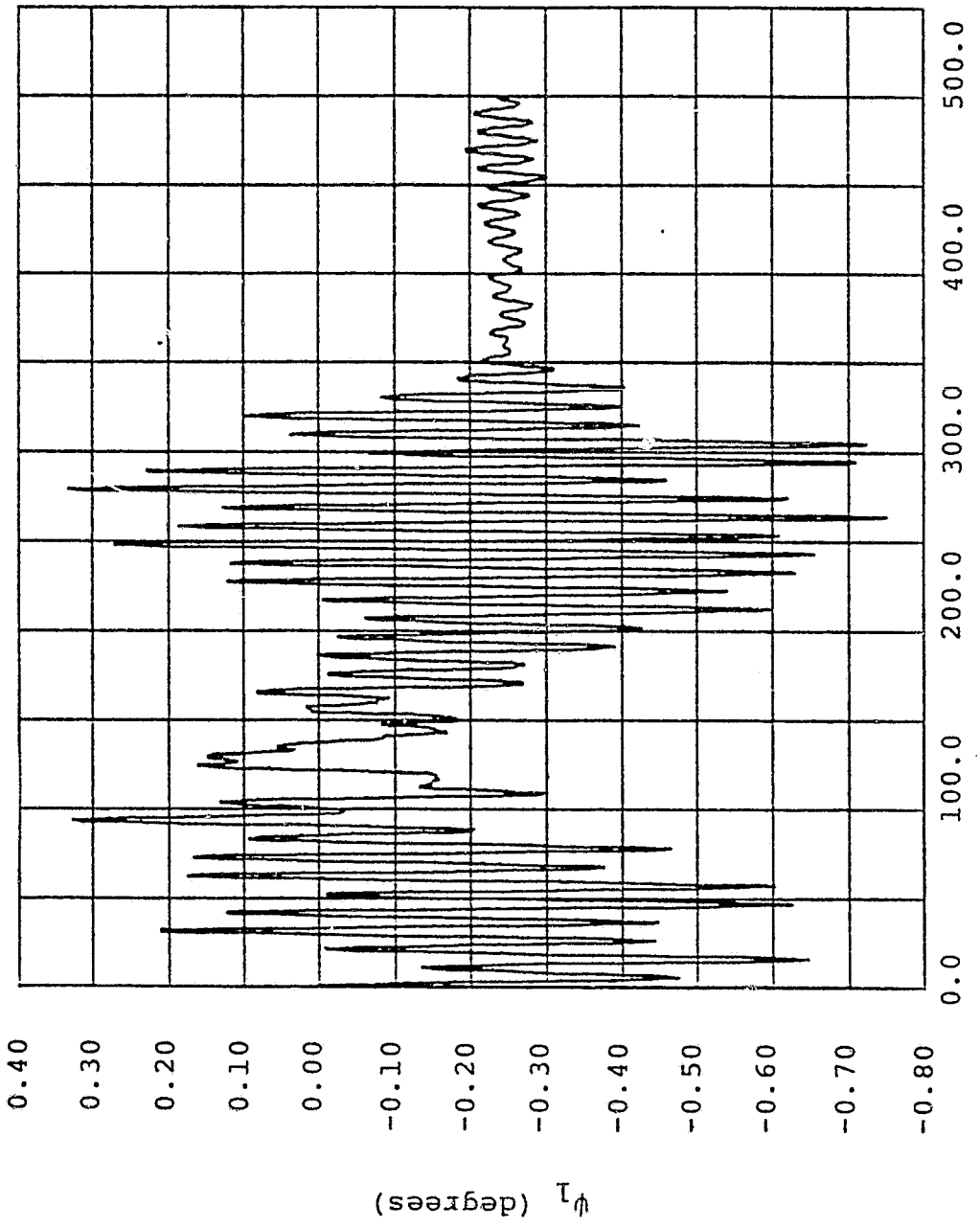

Figure (21) System Response (With Input = a_2)

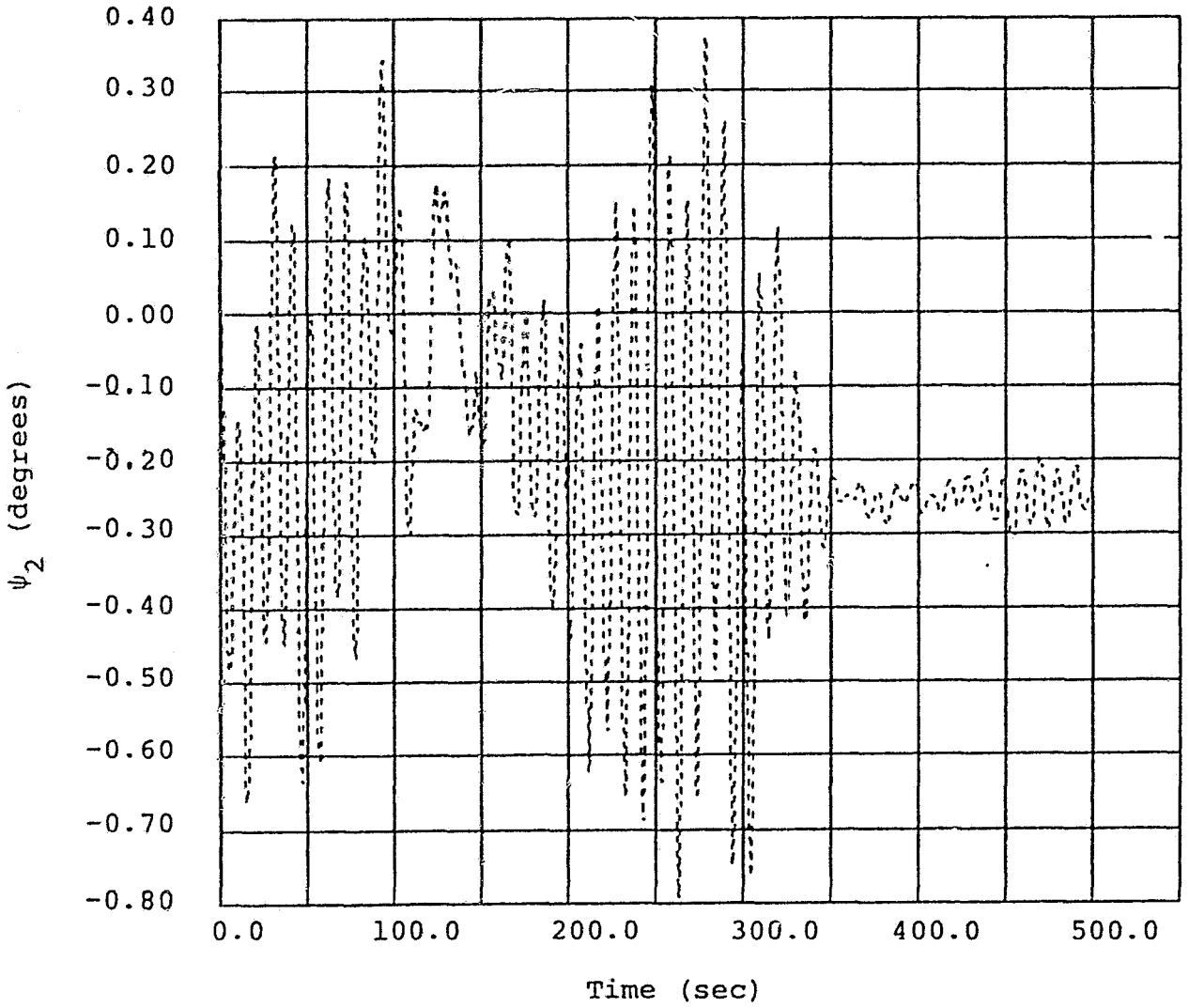

Figure (22) System Response (With Input = a_2)

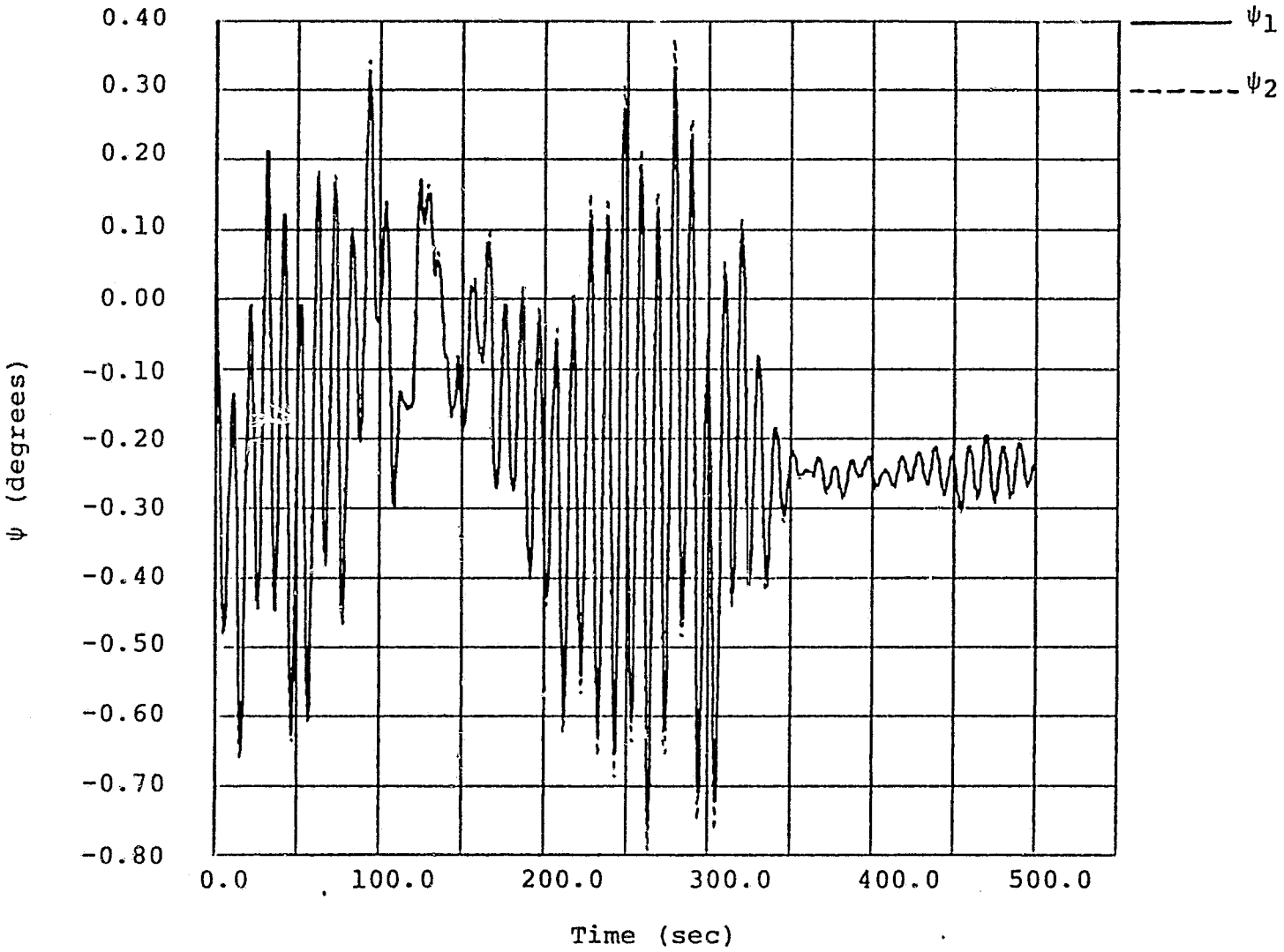

Figure (23) System Response (With Input = a_2)

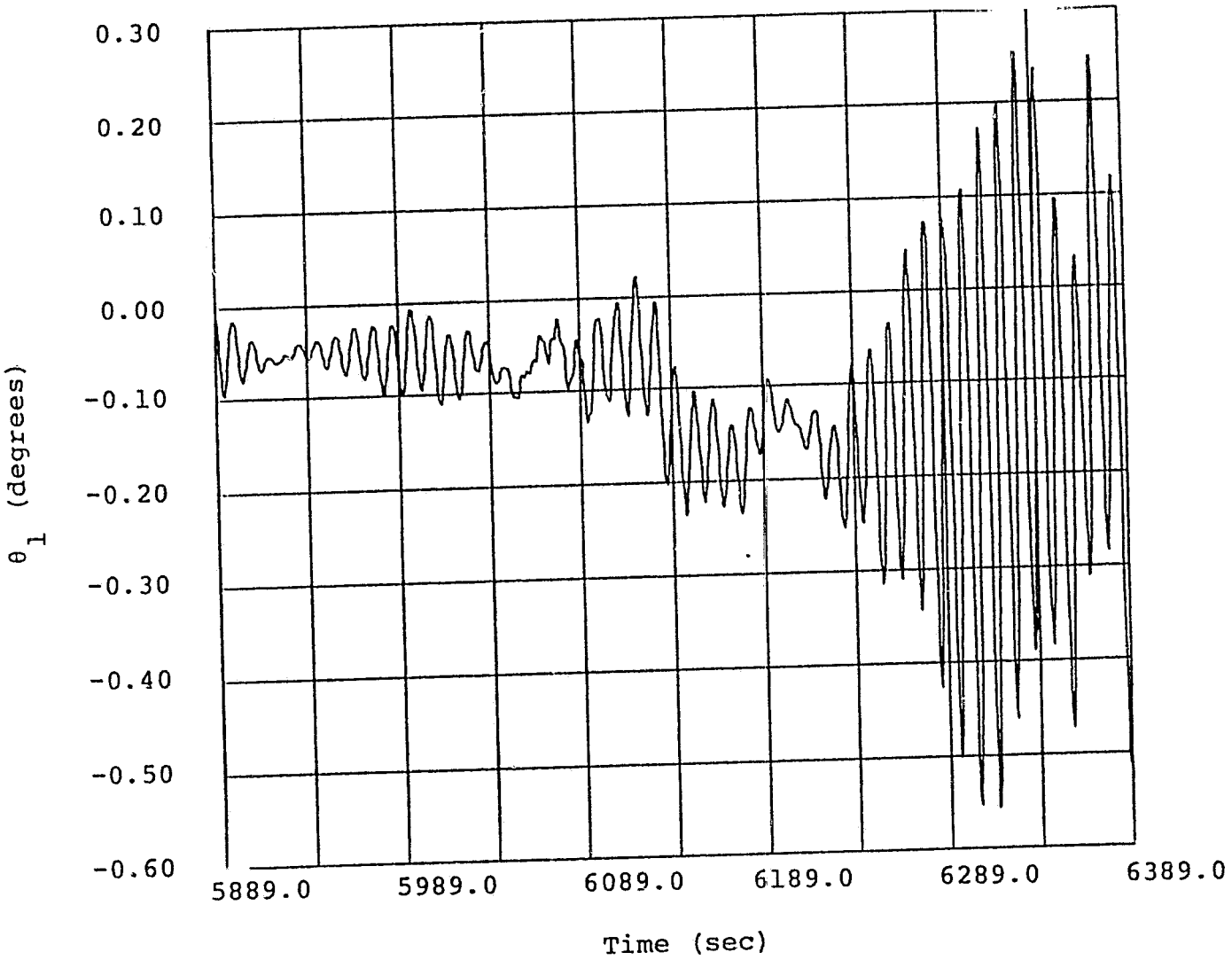

Figure (24) System Response (With Input = a_1)

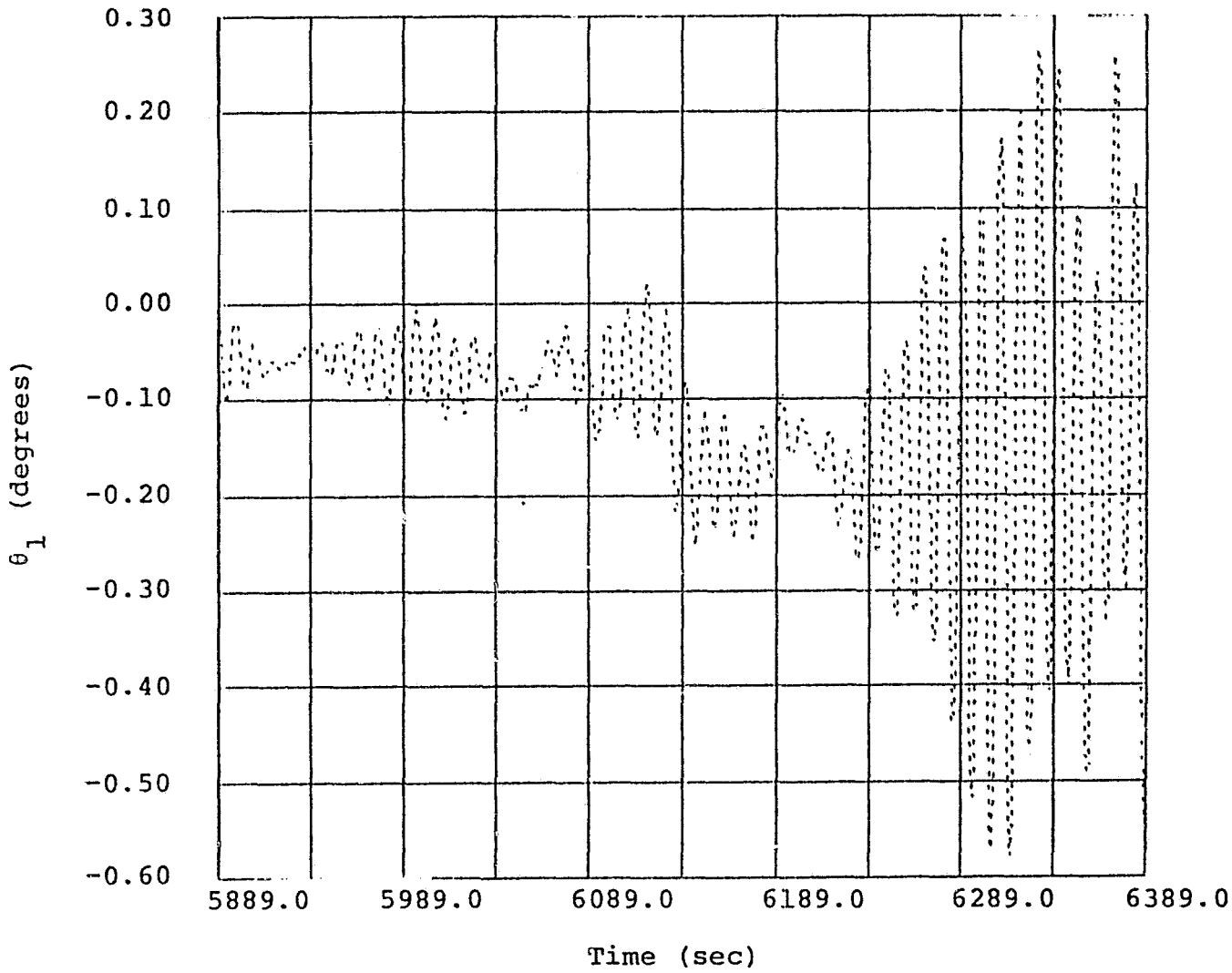

Figure (25) System Response (With Input = a_1)

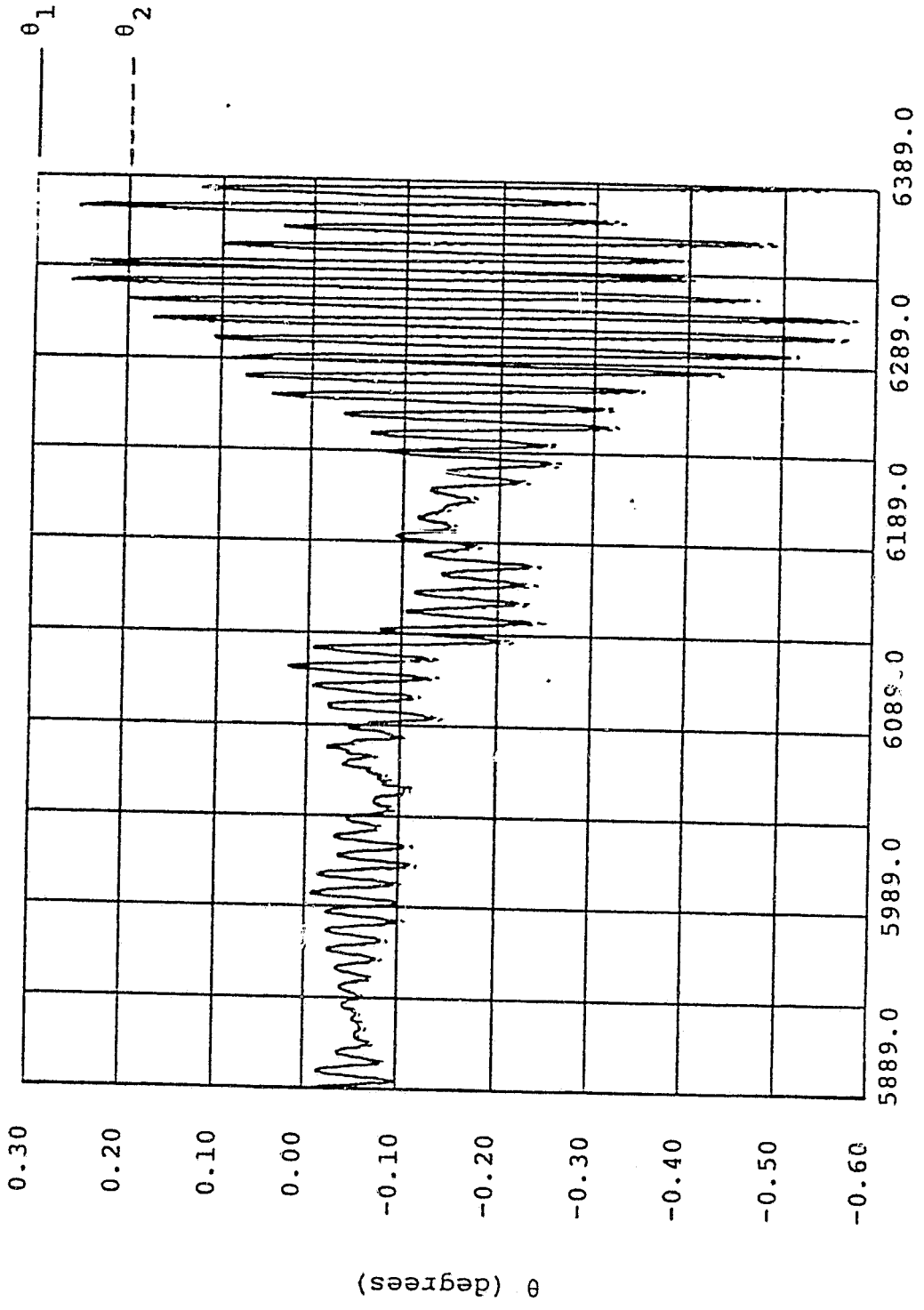

Figure (26) System Response (With Input = a_1)

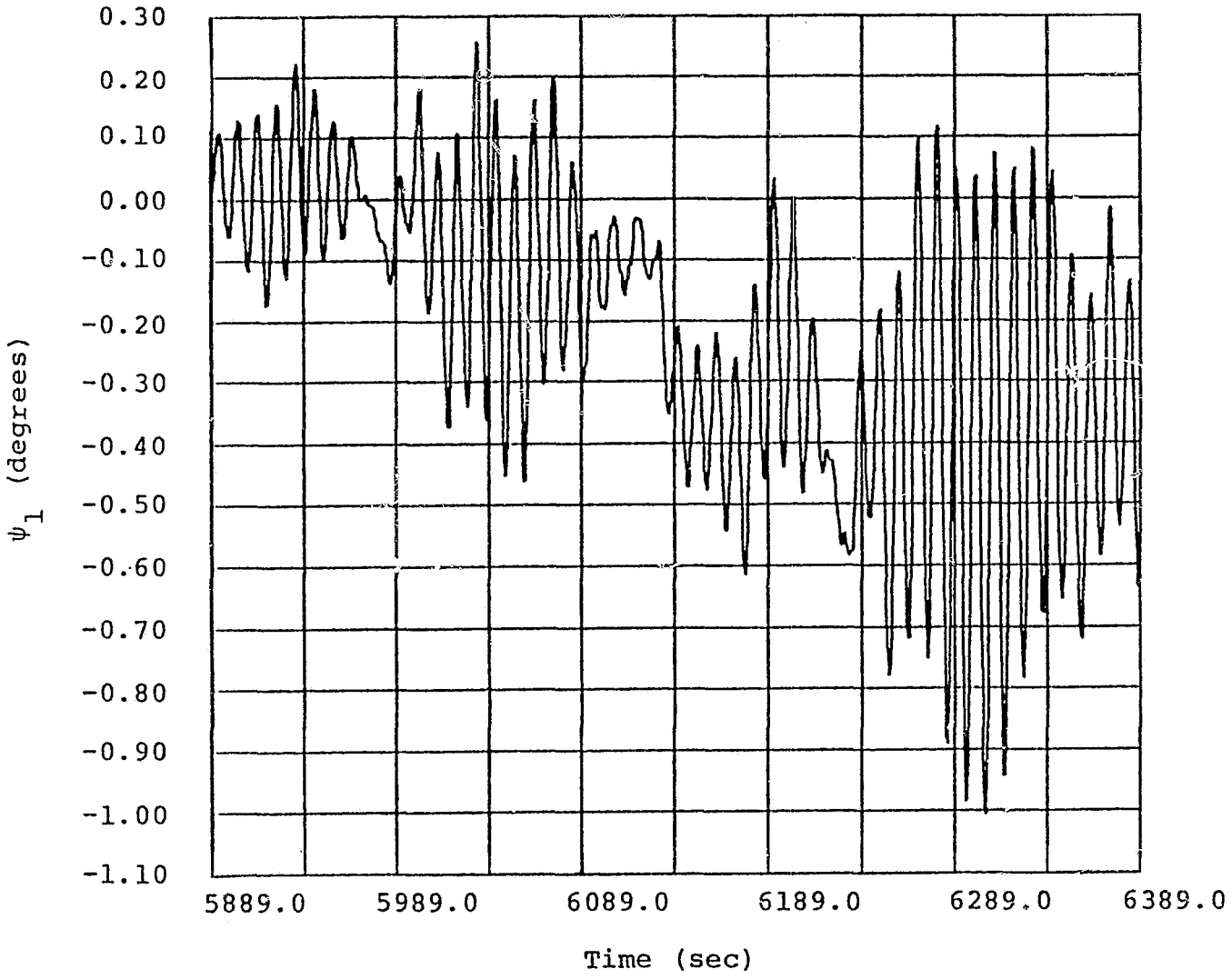

Figure (27) System Response (With Input = a_2)

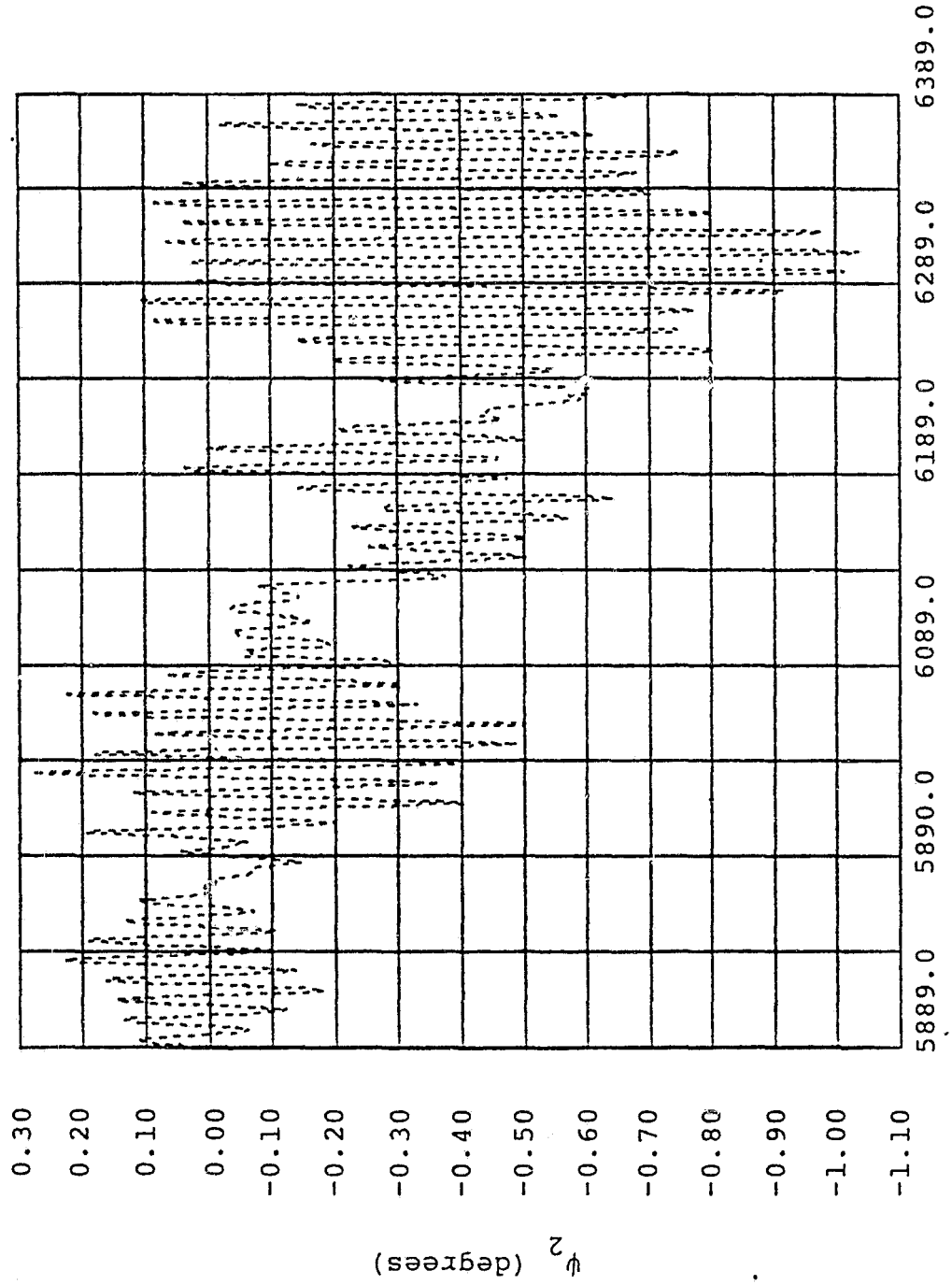

Figure (28) System Response (With Input = a_2)

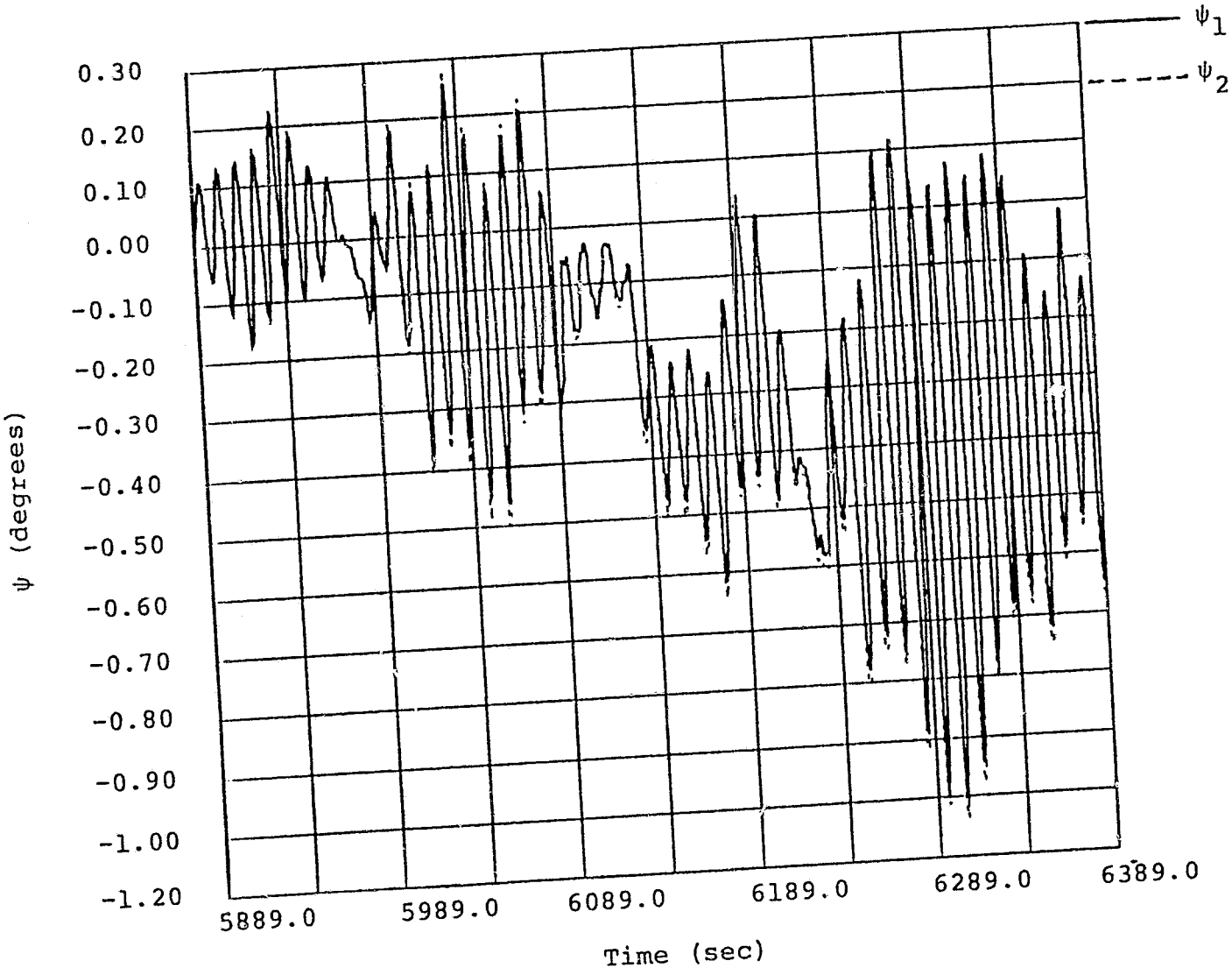

Figure (29) System Response (With Input = a_2)

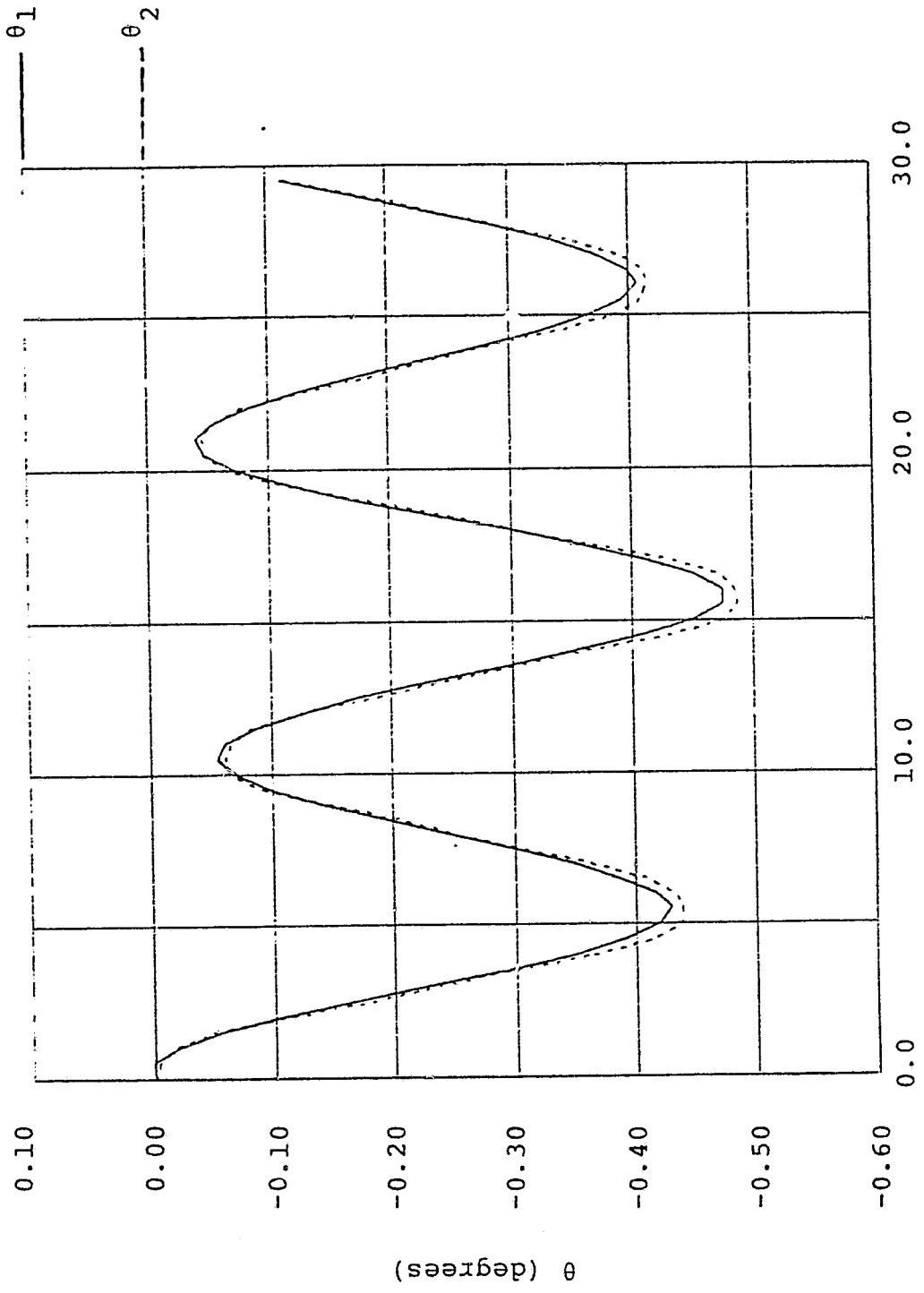

Figure (30) System Response (With Input = a_1)

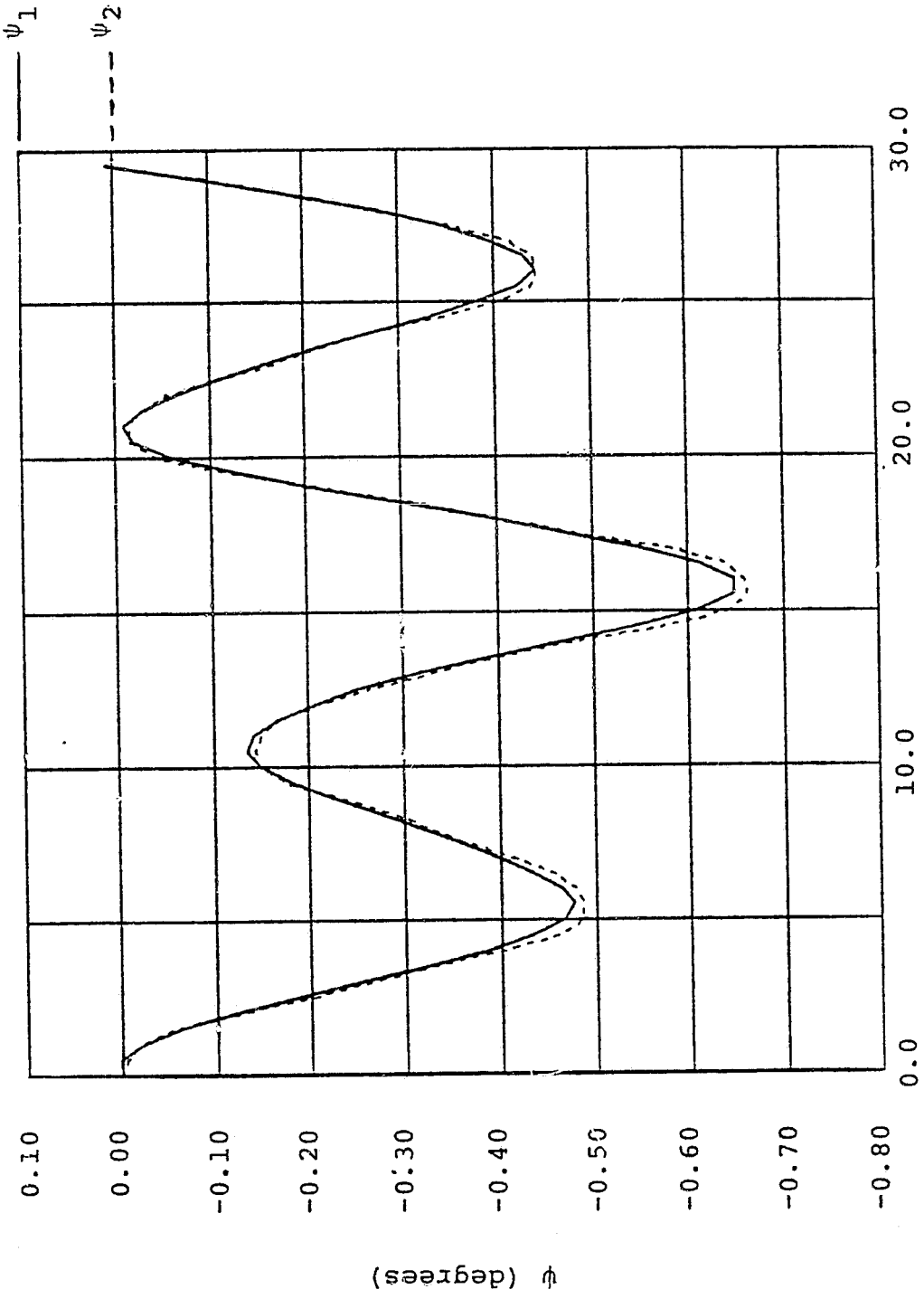

Figure (31) System Response (With Input = a_2)

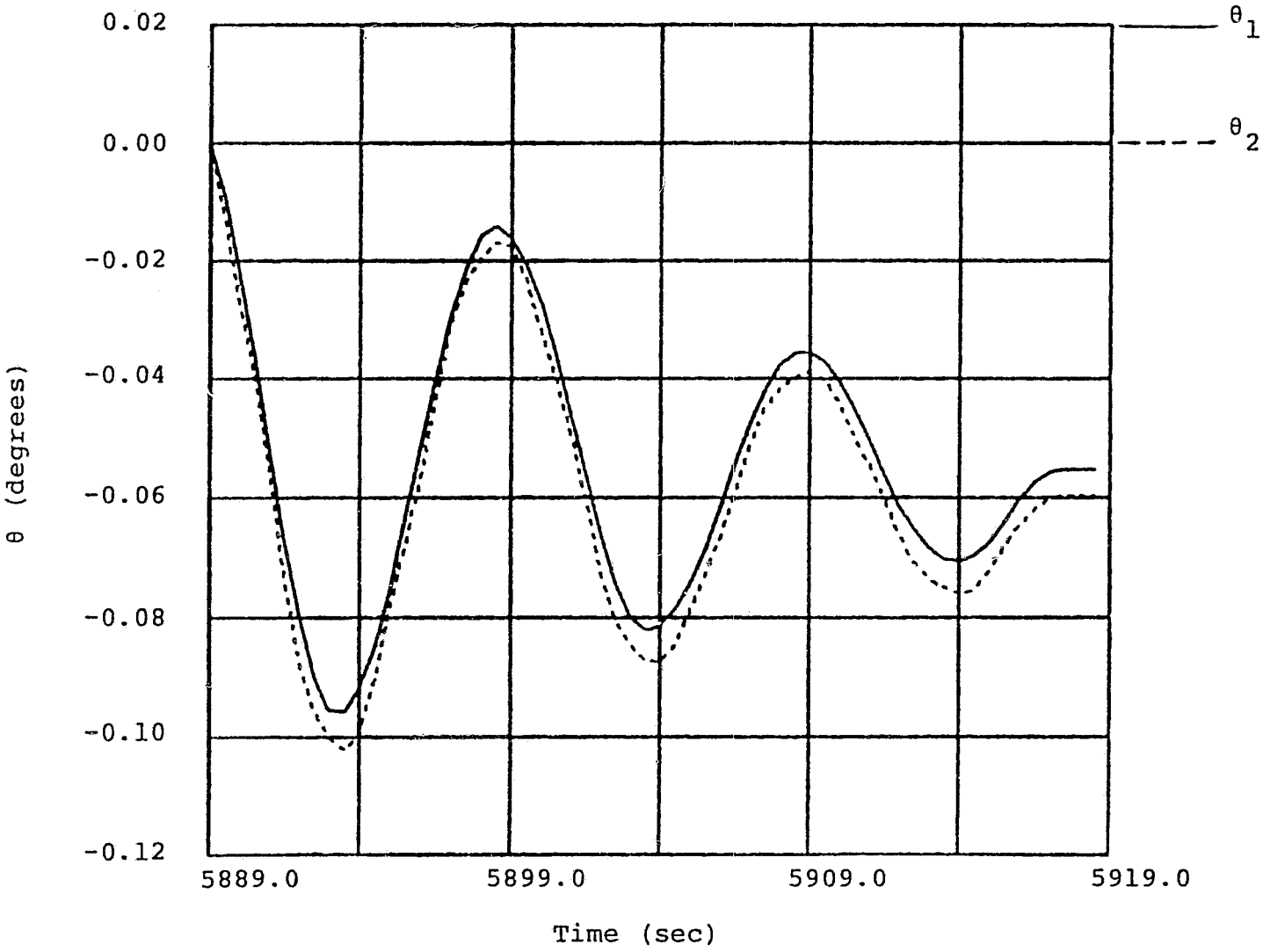

Figure (32) System Response (With Input = a_1)

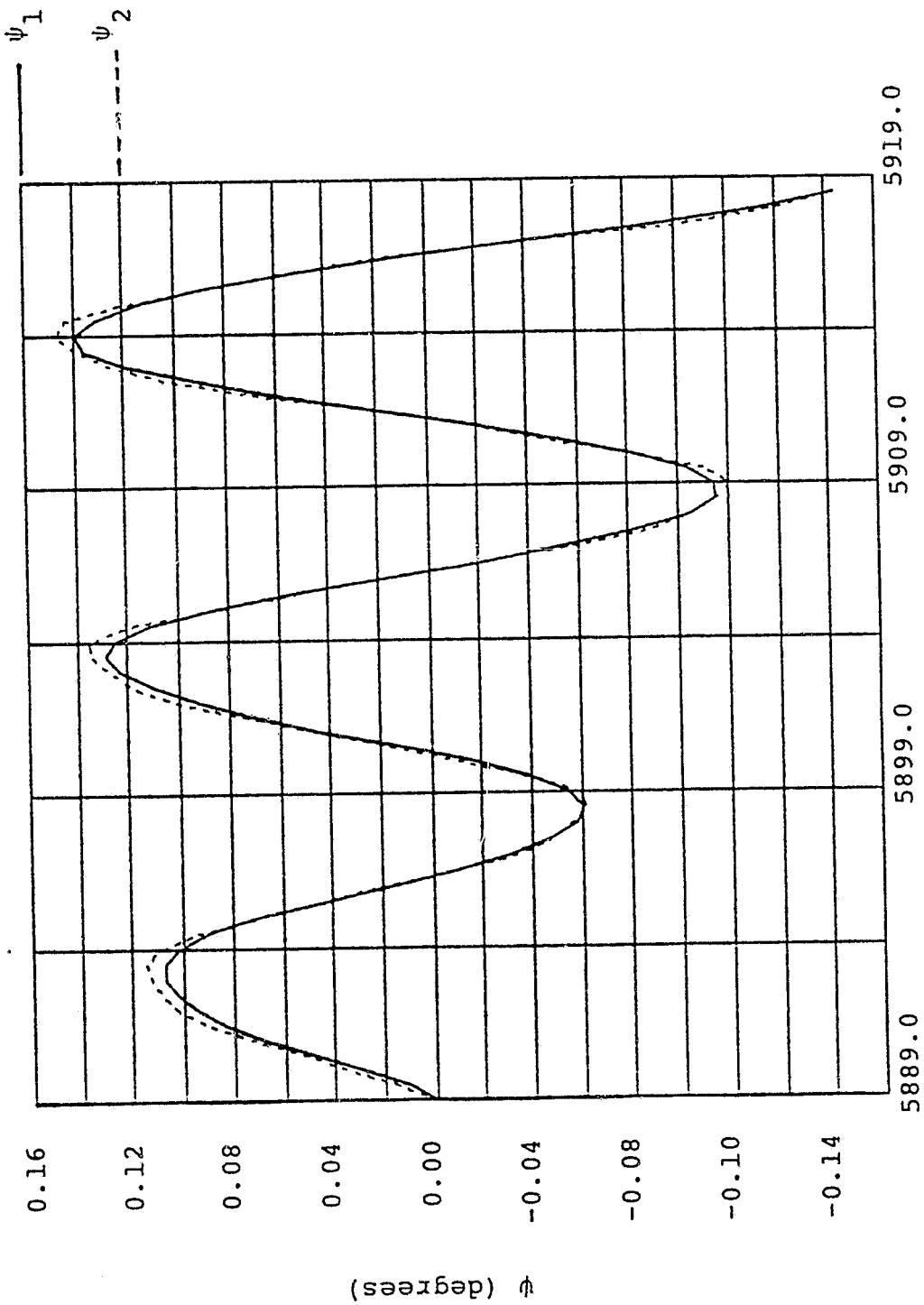

Figure (33) System Response (With Input = a_2)

APPENDIX I

COMPUTER PROGRAM FOR CALCULATING THE FOLLOWING

$\tilde{u}_i$, ω_i, u_{ij}, η_i, θ_i, ψ_i

```
1.000          DIMENSION TIME(1005),P11(1005),P21(1005),X(1001),Y(1001),Z(100
2.000          DIMENSION PDX11(1005),P111(1005),XDOT1(1005),XDOT2(1005)
3.000          DIMENSION P222(1005),X111(1005),Z111(1005),X222(1005),Z222(100
4.000          DIMENSION Y1(1005),Y2(1005),THETA1(1005),THETA2(1005)
5.000          DATA MDIM/1001/
6.000          OUTPUT'INTEGRATION END'
7.000          INPUT  T
8.000          OUTPUT'INPUT WEIGHT 1  (LB)'
9.000          INPUT WEIGHT1
10.000         OUTPUT'INPUT WEIGHT 2  (LB)'
11.000         INPUT WEIGHT2
12.000         OUTPUT'CABLE LENGHT 1  (FT)'
13.000         INPUT CABLEN1
14.000         OUTPUT'CABLE LENGHT 2  (FT)'
15.000         INPUT CABLEN2
16.000         SM1=(WEIGHT1*.4536)/(32.174*.3048)
17.000         SM2=(WEIGHT2*.4536)/(32.174*.3048)
18.000         SL1=CABLEN1*.3048
19.000         SL2=CABLEN2*.3048
20.000         SM11=SL1*SL1*(SM1+SM2)
21.000         SM12=SM2*SL1*SL2
22.000         SM21=SM12
23.000         SM22=SM2*SL2**2
24.000         SK11=32.174*.3048*SL1*(SM1+SM2)
25.000         SK22=32.174*.3048*SM2*SL2
26.000         AAA=.5*(SK11*SM22+SK22*SM11)/(SM11*SM22-SM12*SM21)
27.000         BBB=.5*(((SK11*SM22+SK22*SM11)**2)/(SM11*SM22-SM12
28.000        .*SM21)**2-4*SK11*SK22/(SM11*SM22-SM12*SM21))**.5
29.000         W1SQ=AAA-BBB
30.000         W2SQ=AAA+BBB
31.000         W1=(W1SQ)**.5
32.000         W2=(W2SQ)**.5
33.000         WRITE(101,20)W1,W2
34.000     20  FORMAT(2E14.6)
35.000         CONS1=(SM11+(SK11-W1SQ*SM11)*(SM21+SM12)/(W1SQ*SM12)
36.000        .+(SK11-W1SQ*SM11)**2*SM22/(W1SQ*SM12)**2)**.5
37.000         CONS2=(SM11+(SK11-W2SQ*SM11)*(SM21+SM12)/(W2SQ*SM12)
38.000        .+(SK11-W2SQ*SM11)**2*SM22/(W2SQ*SM12)**2)**.5
39.000 C       CALCULATE EIGENVECTORS
40.000         EIGV11=1.
41.000         EIGV12=1.
42.000         EIGV21=(SK11-W1SQ*SM11)/(W1SQ*SM12)
43.000         EIGV22=(SK11-W2SQ*SM11)/(W2SQ*SM12)
44.000         WRITE(102,30)EIGV11,EIGV12,EIGV21,EIGV22
45.000     30  FORMAT(4E14.6)
46.000 C       CALCULATION OF MODAL MATRIX COMPONENTS NUMERICAL VALUES
47.000         U11=1.0/CONS1
48.000         U12=1.0/CONS2
49.000         U21=(SK11-W1SQ*SM11)/(W1SQ*SM12*CONS1)
50.000         U22=(SK11-W2SQ*SM11)/(W2SQ*SM12*CONS2)
```

```
      WRITE(105,40)U11,U12,U21,U22
   40 FORMAT(4E14.6)
C     INPUT DATA FILE
      DO 55 J=1,1001
   55 READ(103,150)          TIME(J),XDDOT1(J),XDDOT2(J)
  150 FORMAT(3E14.6)
      DO 70 I=1,1001
      E11(I)=-(SM1*CL1+SM2*CL1)*XDDOT1(I)
      E21(I)=-SM2*CL2*XDDOT1(I)
   70 CONTINUE
      DO 50 J=1,1001
      E111(J)=E11(J)*U11+E21(J)*U21
      E222(J)=E11(J)*U12+E21(J)*U22
C     CALCULATE EOA VALUES INPUT(A1)
   50 CONTINUE
      DO 80 J=1,1001
      EUN11(J)=SIN(W1*(T-TIME(J)))*E111(J)/W1
      Y(J)=EUN11(J)
      X(J)=TIME(J)
   80 CONTINUE
      CALL EPSXY(X,Y,Z,NDIM)
      DO 140 J=1,1001
      X111(J)=X(J)
      Z111(J)=Z(J)
  140 WRITE(106,141)X111(J),Z111(J)
  141 FORMAT(2E14.6)
      DO 180 J=1,1001
      EUN11(J)=SIN(W2*(T-TIME(J)))*E222(J)/W2
      Y(J)=EUN11(J)
      X(J)=TIME(J)
  180 CONTINUE
      CALL EPSXY(X,Y,Z,NDIM)
      DO 145 J=1,1001
      X222(J)=X(J)
      Z222(J)=Z(J)
  145 WRITE(104,146)X222(J),Z222(J)
  146 FORMAT(2E14.6)
C     CALCULATE SYSTEM RESPONSE INPUT (A1)
      DO 210 I=1,1001
      X1(I)=U11*Z111(I)+U12*Z222(I)
      X2(I)=U21*Z111(I)+U22*Z222(I)
      WRITE(109,200)TIME(I),X1(I),X2(I)
  200 FORMAT(3E14.6)
  210 CONTINUE
      DO 310 I=1,1001
      THETA1(I)=180.0*X1(I)/3.14159265
      THETA2(I)=180.0*X2(I)/3.14159265
      WRITE(112,320)TIME(I),THETA1(I),THETA2(I)
  320 FORMAT(3E14.6)
  310 CONTINUE
      DO 71 I=1,1001
      E11(I)=-(SM1*CL1+SM2*CL1)*XDDOT2(I)
```

```
103.000          P21(I)=-SM2*PL2*XDOT2(I)
104.000       71 CONTINUE
105.000          DO 51 J=1,1001
106.000          P111(J)=P11(J)*H11+P21(J)*H21
107.000          P222(J)=P11(J)*H12+P21(J)*H22
108.000       51 CONTINUE
109.000 C        CALCULATE RTA VALUES INPUT (A2)
110.000          DO 81 J=1,1001
111.000          FUN11(J)=SIN(W1*(T-TIME(J)))*P111(J)/W1
112.000          Y(J)=FUN11(J)
113.000          X(J)=TIME(J)
114.000       81 CONTINUE
115.000          CALL TPZXY(X,Y,Z,NDIM)
116.000          DO 143 J=1,1001
117.000          X111(J)=X(J)
118.000          Z111(J)=Z(J)
119.000      143 WRITE(107,142)X111(J),Z111(J)
120.000      142 FORMAT(2E14.6)
121.000          DO 181 J=1,1001
122.000          FUN11(J)=SIN(W2*(T-TIME(J)))*P222(J)/W2
123.000          Y(J)=FUN11(J)
124.000          X(J)=TIME(J)
125.000      181 CONTINUE
126.000          CALL TPZXY(X,Y,Z,NDIM)
127.000          DO 148 J=1,1001
128.000          X222(J)=Y(J)
129.000          Z222(J)=Z(J)
130.000      148 WRITE(111,149)X222(J),Z222(J)
131.000      149 FORMAT(2E14.6)
132.000 C        CALCULATE SYSTEM RESPONSE INPUT (A2)
133.000          DO 211 I=1,1001
134.000          X1(I)=H11*Z111(I)+H12*Z222(I)
135.000          X2(I)=H21*Z111(I)+H22*Z222(I)
136.000          WRITE(110,300)TIME(I),X1(I),X2(I)
137.000      300 FORMAT(3E14.6)
138.000      211 CONTINUE
139.000          DO 400 I=1,1001
140.000          THETA1(I)=180.0*X1(I)/3.14159265
141.000          THETA2(I)=180.0*X2(I)/3.14159265
142.000          WRITE(113,420)TIME(I),THETA1(I),THETA2(I)
143.000      420 FORMAT(3E14.6)
144.000      400 CONTINUE
145.000          STOP
146.000          END
*
```

APPENDIX II

COMPUTER PROGRAM FOR CALCULATING VALUES OF η_1 FROM ANALYTICALLY INTEGRATED EQUATION

```
 1.000        DIMENSION PHI(2000),T(2000)
 2.000        T1=200
 3.000        P=4.2467
 4.000        T(1)=0
 5.000        W1=.60063
 6.000        DO 50 I=1,400
 7.000        PHI(I)=.0002*P*T(I)*COS(W1*(T1-T(I)))/W1**2
 8.000       .+.0002*P*SIN(W1*(T1-T(I)))/W1**3
 9.000       .-.0002*P*SIN(W1*T1)/W1**3
10.000       .-.04*P*COS(W1*(T1-T(I)))/W1**2
11.000       .+.04*P*COS(W1*T1)/W1**2
12.000    50 T(I+1)=T(I)+.5
13.000        DO 10 I=1,400
14.000    10 WRITE(108,100) T(I),PHI(I)
15.000   100 FORMAT(2E14.6)
16.000        STOP
17.000        END
*
```

BIBLIOGRAPHY

1. Foot, J.L., Simmons, E.L., and Whittaker, A.E., "Measurements of the Swing of a Balloon Payload," Meteorlogical Magazine, 103, pg 110-112, 1974.

2. Peltifer, R.E., and Flavell, R.G., "Some Aspects of the Swinging of Balloon Borne Payloads," Meteorlogical Magazine, 105, pg 194-205.

3. Nigro, N.J., Elkouh, A.F., et. al., "Attitude Determination of a High Altitude Balloon System. Part I: Development of the Mathematical Model," NASA Report CR-142193, 1975

4. Gagliardi, J.C., "Feasibility of Observer System for Determining Orientation of Balloon Borne Observational Platform," M.S. Thesis, Marquette University, 1982

5. Meirovitch, L., Analytical Methods in Vibrations, New York: The MacMillan Company, 1967